

Status of the analysis of $^{94,95,96}\text{Mo}(n,\gamma)$

RICCARDO MUCCIOLA

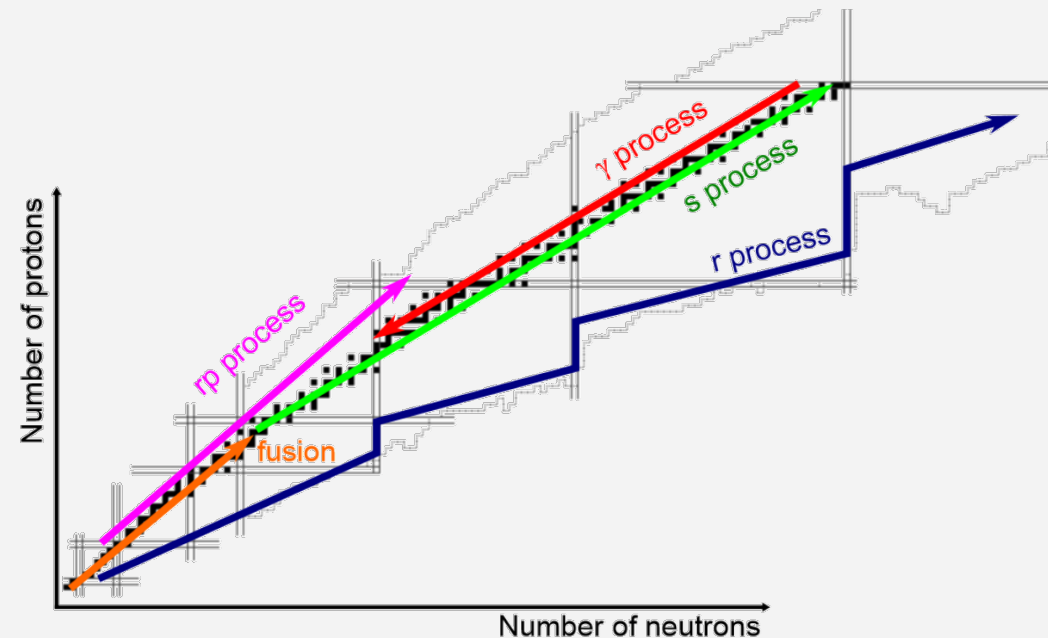
Importance of molybdenum



- Fission product in nuclear power plants;
- Transport casks, irradiated fuel storage;
- Research reactors and Accident Tolerant Fuels;
- Stellar nucleosynthesis;

Stellar nucleosynthesis

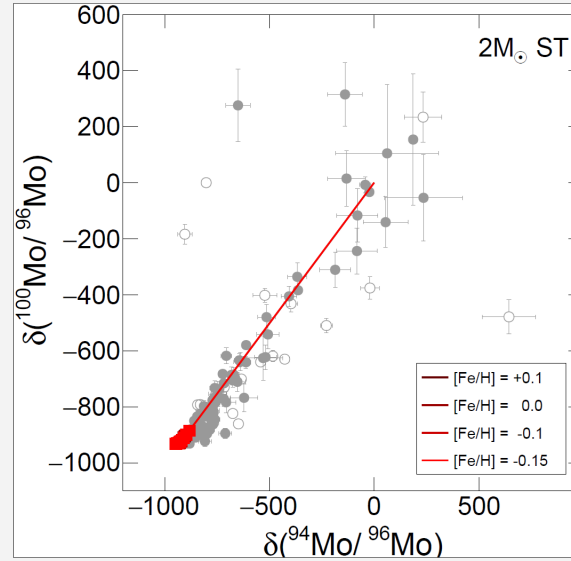
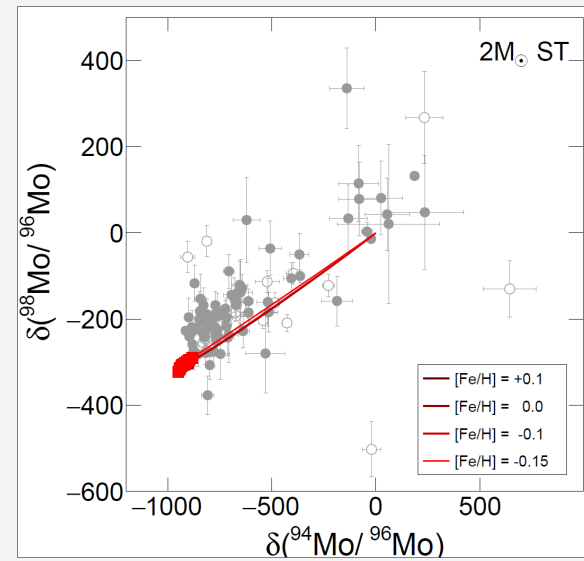
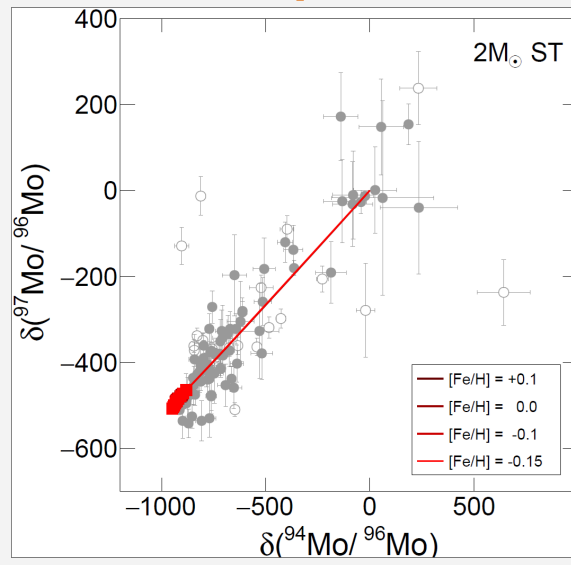
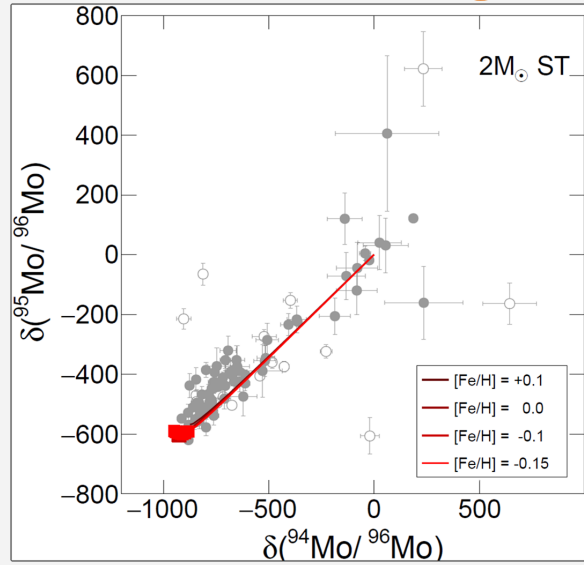
- Four main nucleosynthesis processes for elements heavier than iron: **s-process**, r-process, i-process, and p-process;
- Some isotopes can be synthesized only by one process (e.g., ^{96}Mo by s-process);
- Possible to set constraints on intensity of the processes.



s-process path around molybdenum

$^{94}_{44}\text{Ru}_{50}$ Stable 0+ $\Delta = -86241$ $\beta = 100\%$	$^{95}_{44}\text{Ru}_{51}$ Stable 5/2+ $\Delta = -83458$ $\beta = 100\%$	$^{96}_{44}\text{Ru}_{52}$ Stable >80Eγ 0+ $\Delta = -86080$ $\beta = 100\%$	$^{97}_{44}\text{Ru}_{53}$ Stable 5/2+ $\Delta = -86120$ $\beta = 100\%$	$^{98}_{44}\text{Ru}_{54}$ Stable 0+ $\Delta = -88225$ $\beta = 100\%$	$^{99}_{44}\text{Ru}_{55}$ Stable 5/2+ $\Delta = -87625$ $\beta = 100\%$	$^{100}_{44}\text{Ru}_{56}$ Stable 0+ $\Delta = -89227$ $\beta = 100\%$	$^{101}_{44}\text{Ru}_{57}$ Stable 5/2+ $\Delta = -87914$ $\beta = 100\%$	$^{102}_{44}\text{Ru}_{58}$ Stable 0+ $\Delta = -89106$ $\beta = 100\%$
$^{93}_{43}\text{Tc}_{50}$ Stable 5/2+ $\Delta = -87461$ $\beta = 100\%$	$^{94}_{43}\text{Tc}_{51}$ Stable 5/2+ $\Delta = -86013$ $\beta = 100\%$	$^{95}_{43}\text{Tc}_{52}$ Stable 5/2+ $\Delta = -86113$ $\beta = 100\%$	$^{96}_{43}\text{Tc}_{53}$ Stable 5/2+ $\Delta = -86113$ $\beta = 100\%$	$^{97}_{43}\text{Tc}_{54}$ Stable 5/2+ $\Delta = -86013$ $\beta = 100\%$	$^{98}_{43}\text{Tc}_{55}$ Stable 5/2+ $\Delta = -86013$ $\beta = 100\%$	$^{99}_{43}\text{Tc}_{56}$ Stable 5/2+ $\Delta = -86013$ $\beta = 100\%$	$^{100}_{43}\text{Tc}_{57}$ Stable 5/2+ $\Delta = -86013$ $\beta = 100\%$	$^{101}_{43}\text{Tc}_{58}$ Stable 5/2+ $\Delta = -86013$ $\beta = 100\%$
$^{92}_{42}\text{Mo}_{50}$ Stable 0+ $\Delta = -86113$ $\beta = 100\%$	$^{93}_{42}\text{Mo}_{51}$ Stable 5/2+ $\Delta = -86113$ $\beta = 100\%$	$^{94}_{42}\text{Mo}_{52}$ Stable 5/2+ $\Delta = -86113$ $\beta = 100\%$	$^{95}_{42}\text{Mo}_{53}$ Stable 5/2+ $\Delta = -86113$ $\beta = 100\%$	$^{96}_{42}\text{Mo}_{54}$ Stable 5/2+ $\Delta = -86113$ $\beta = 100\%$	$^{97}_{42}\text{Mo}_{55}$ Stable 5/2+ $\Delta = -86113$ $\beta = 100\%$	$^{98}_{42}\text{Mo}_{56}$ Stable 5/2+ $\Delta = -86113$ $\beta = 100\%$	$^{99}_{42}\text{Mo}_{57}$ Stable 5/2+ $\Delta = -86113$ $\beta = 100\%$	$^{100}_{42}\text{Mo}_{58}$ Stable 5/2+ $\Delta = -86113$ $\beta = 100\%$
$^{91}_{41}\text{Nb}_{50}$ Stable 5/2+ $\Delta = -86113$ $\beta = 100\%$	$^{92}_{41}\text{Nb}_{51}$ Stable 5/2+ $\Delta = -86113$ $\beta = 100\%$	$^{93}_{41}\text{Nb}_{52}$ Stable 5/2+ $\Delta = -86113$ $\beta = 100\%$	$^{94}_{41}\text{Nb}_{53}$ Stable 5/2+ $\Delta = -86113$ $\beta = 100\%$	$^{95}_{41}\text{Nb}_{54}$ Stable 5/2+ $\Delta = -86113$ $\beta = 100\%$	$^{96}_{41}\text{Nb}_{55}$ Stable 5/2+ $\Delta = -86113$ $\beta = 100\%$	$^{97}_{41}\text{Nb}_{56}$ Stable 5/2+ $\Delta = -86113$ $\beta = 100\%$	$^{98}_{41}\text{Nb}_{57}$ Stable 5/2+ $\Delta = -86113$ $\beta = 100\%$	$^{99}_{41}\text{Nb}_{58}$ Stable 5/2+ $\Delta = -86113$ $\beta = 100\%$
$^{90}_{40}\text{Zr}_{50}$ Stable 0+ $\Delta = -86113$ $\beta = 100\%$	$^{91}_{40}\text{Zr}_{51}$ Stable 5/2+ $\Delta = -86113$ $\beta = 100\%$	$^{92}_{40}\text{Zr}_{52}$ Stable 5/2+ $\Delta = -86113$ $\beta = 100\%$	$^{93}_{40}\text{Zr}_{53}$ Stable 5/2+ $\Delta = -86113$ $\beta = 100\%$	$^{94}_{40}\text{Zr}_{54}$ Stable 5/2+ $\Delta = -86113$ $\beta = 100\%$	$^{95}_{40}\text{Zr}_{55}$ Stable 5/2+ $\Delta = -86113$ $\beta = 100\%$	$^{96}_{40}\text{Zr}_{56}$ Stable 5/2+ $\Delta = -86113$ $\beta = 100\%$	$^{97}_{40}\text{Zr}_{57}$ Stable 5/2+ $\Delta = -86113$ $\beta = 100\%$	$^{98}_{40}\text{Zr}_{58}$ Stable 5/2+ $\Delta = -86113$ $\beta = 100\%$

Presolar grain composition



- Comparison of SiC grains composition versus stellar model (FRANEC) using delta notation:

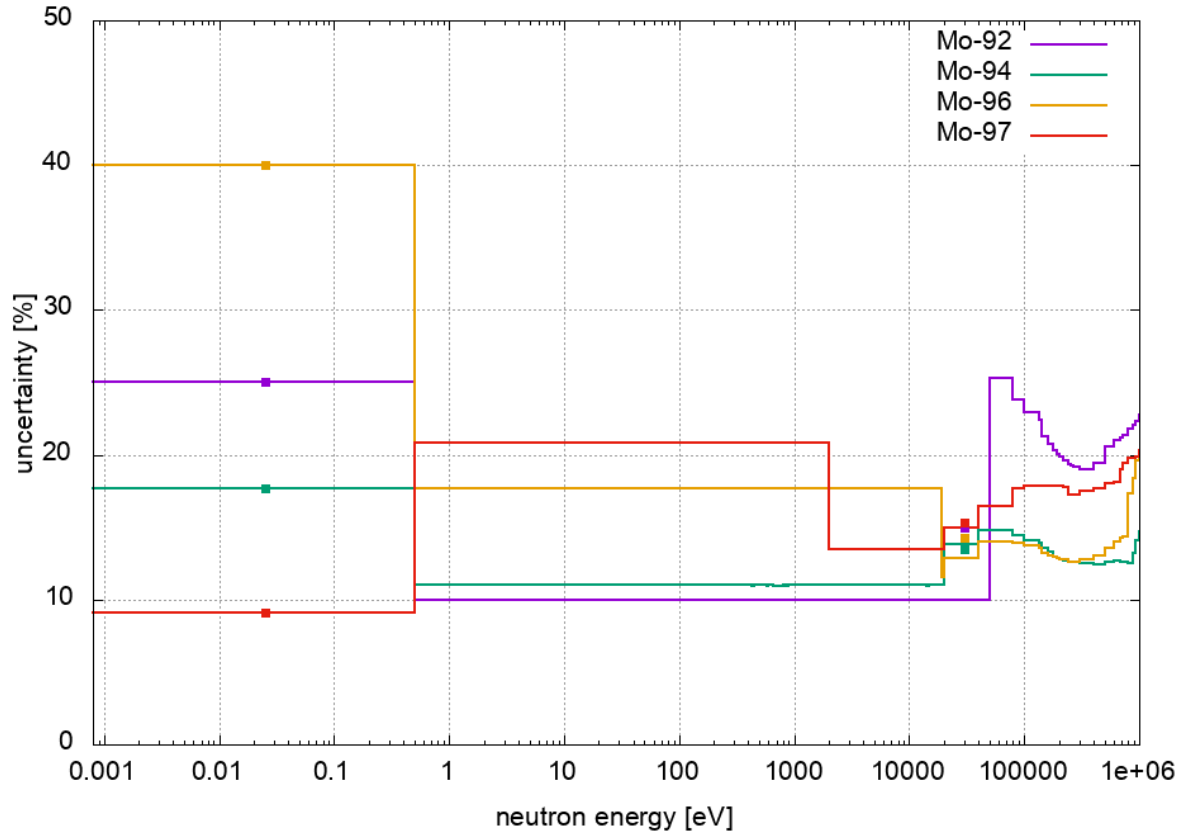
$$\delta \left(\frac{{}^{95}\text{Mo}}{{}^{96}\text{Mo}} \right) = 10^3 \times \left[\frac{\left(\frac{{}^{95}\text{Mo}}{{}^{96}\text{Mo}} \right)}{\left(\frac{{}^{95}\text{Mo}}{{}^{96}\text{Mo}} \right)_\odot} - 1 \right]$$

- MACS from KADoNiS v1.0 database,
- Slight discrepancies between model and isotopic composition,
- Possible overestimation of MACS in KADoNiS.

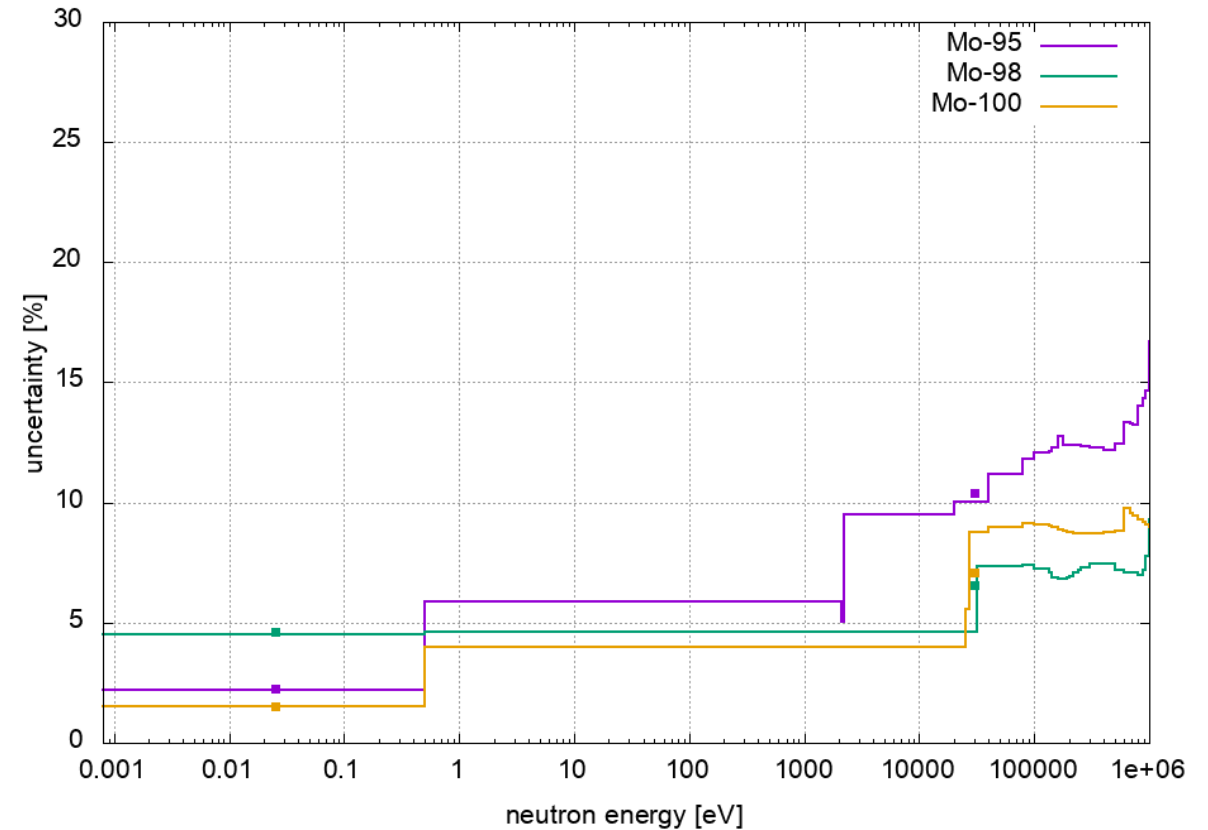
S. Palmerini et al., ApJ 921 7 (2021)

Cross section uncertainties in ENDF/B-VIII

Capture cross section uncertainties - ENDF/B-VIII.0 data set

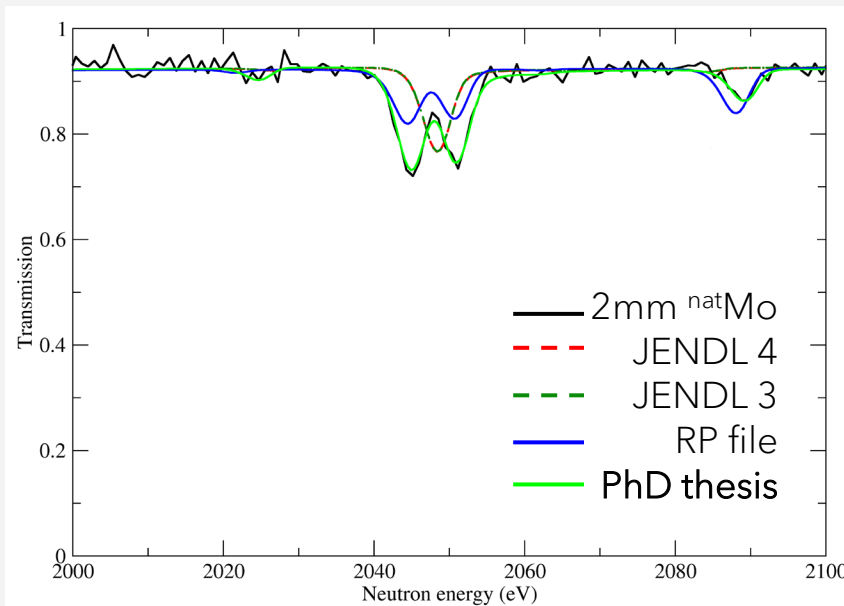
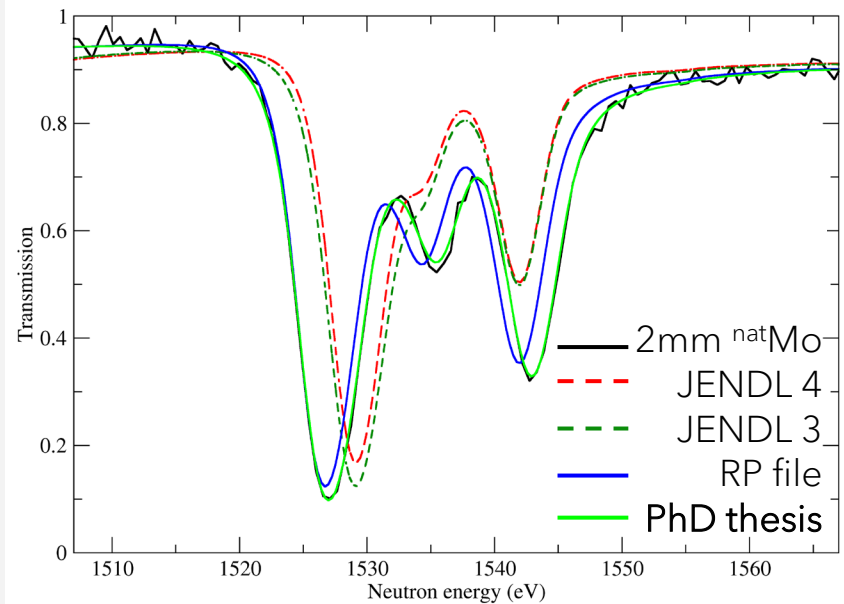


Capture cross section uncertainties - ENDF/B-VIII.0 data set



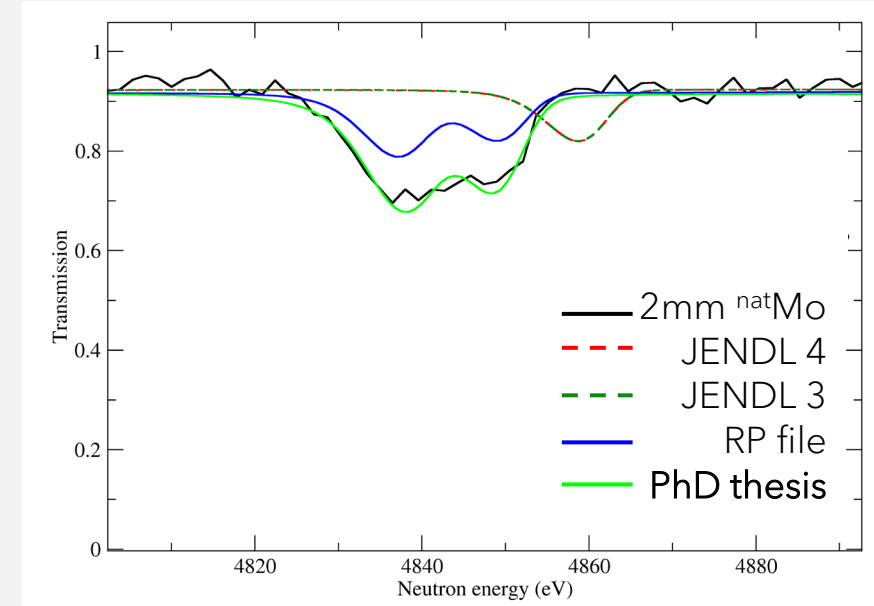
ENDF/B-VIII: D. Brown et al., Nucl. Data. Sheets 148 (2012)

Improvement of RP file



- RP file improved by an adjustment to transmission data using REFIT
- Fit of resonances up to 5 keV
- Details showed in [last Collaboration meeting](#)

R. Mucciola et al., NIMB 531 (2022) 100



n_TOF measurements

Last meeting

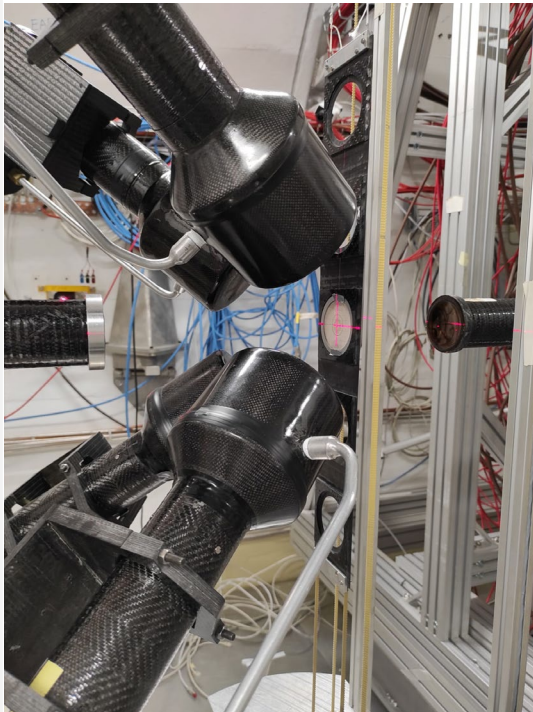
This talk

EAR2_2021	EAR1_2022	EAR2_2022
1.7 10^{18} protons	6.0 10^{18} protons	1.7 10^{18} protons
3 B6D6, 1 L6D6, 1 STED	4 C6D6	8 STED, 2 L6D6, 1 DSTI
Powder sample in aluminum canning	Pressed pellets in plastic bags	Pressed pellets in plastic bags

+ additional transmission measurement with enriched pellets at 10m station of GELINA
+ transmission measurements with natural samples at 50m station of GELINA

Experimental conditions @ EAR1

DETECTION SETUP



Setup:

- 4 C6D6,
- 8 cm from sample.

SAMPLES



Samples:

- Pressed pellets in thin plastic bags,
- Samples mounted in sample exchanger.

Background estimation

Background of capture measurements

The background of a capture measurements can be expressed as:

$$B = b_0 + b_s(t) + b_n(t) + b_\gamma(t)$$

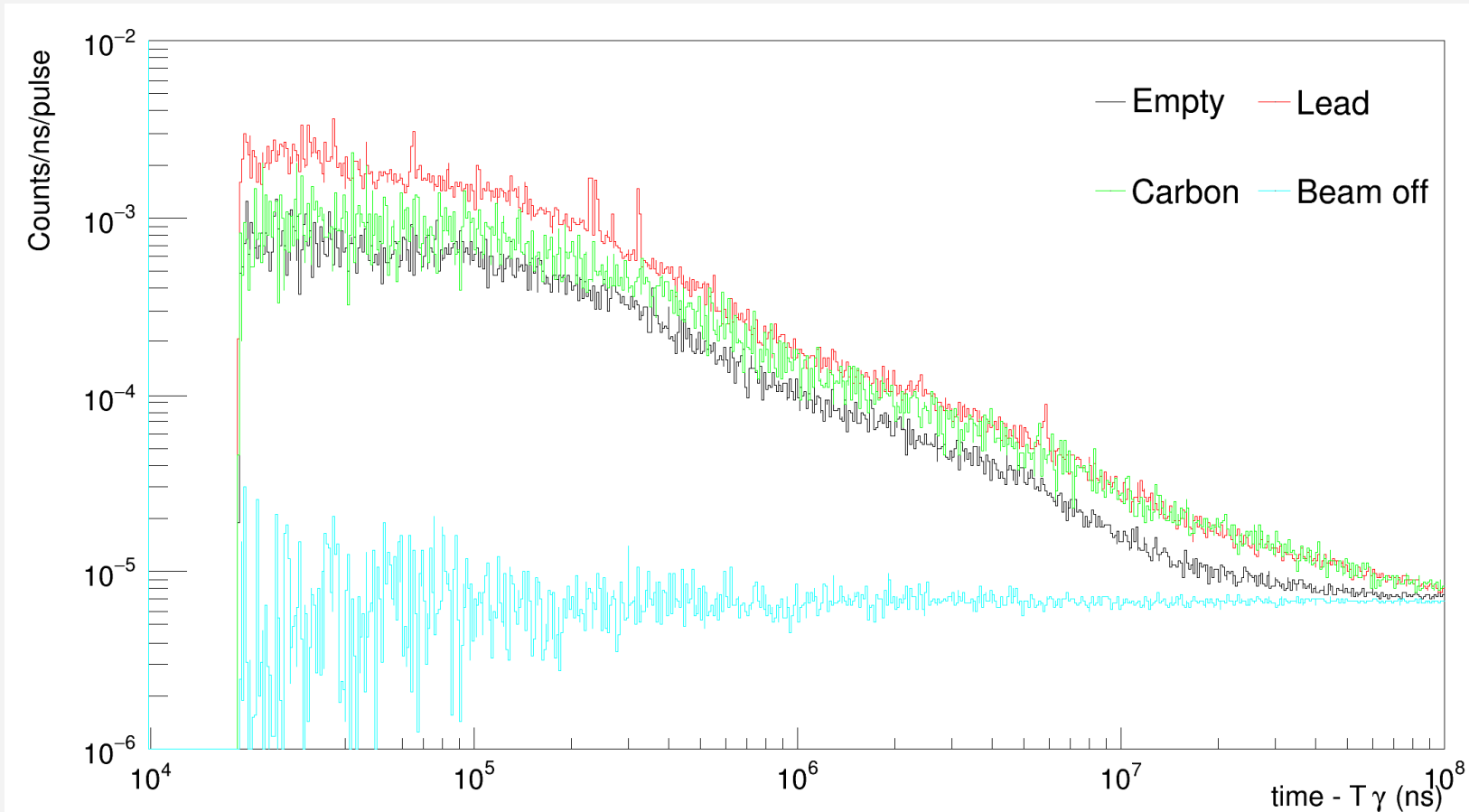
Where b_0 is the time independent background, $b_s(t)$ is the time-dependent sample-independent background, $b_n(t)$ is the sample dependent neutron scattering and $b_\gamma(t)$ is the sample dependent in-beam gamma scattering.

b_0 can be estimated with a beam-off measurement;

$b_s(t)$ can be estimated with a measurement with an empty sample;

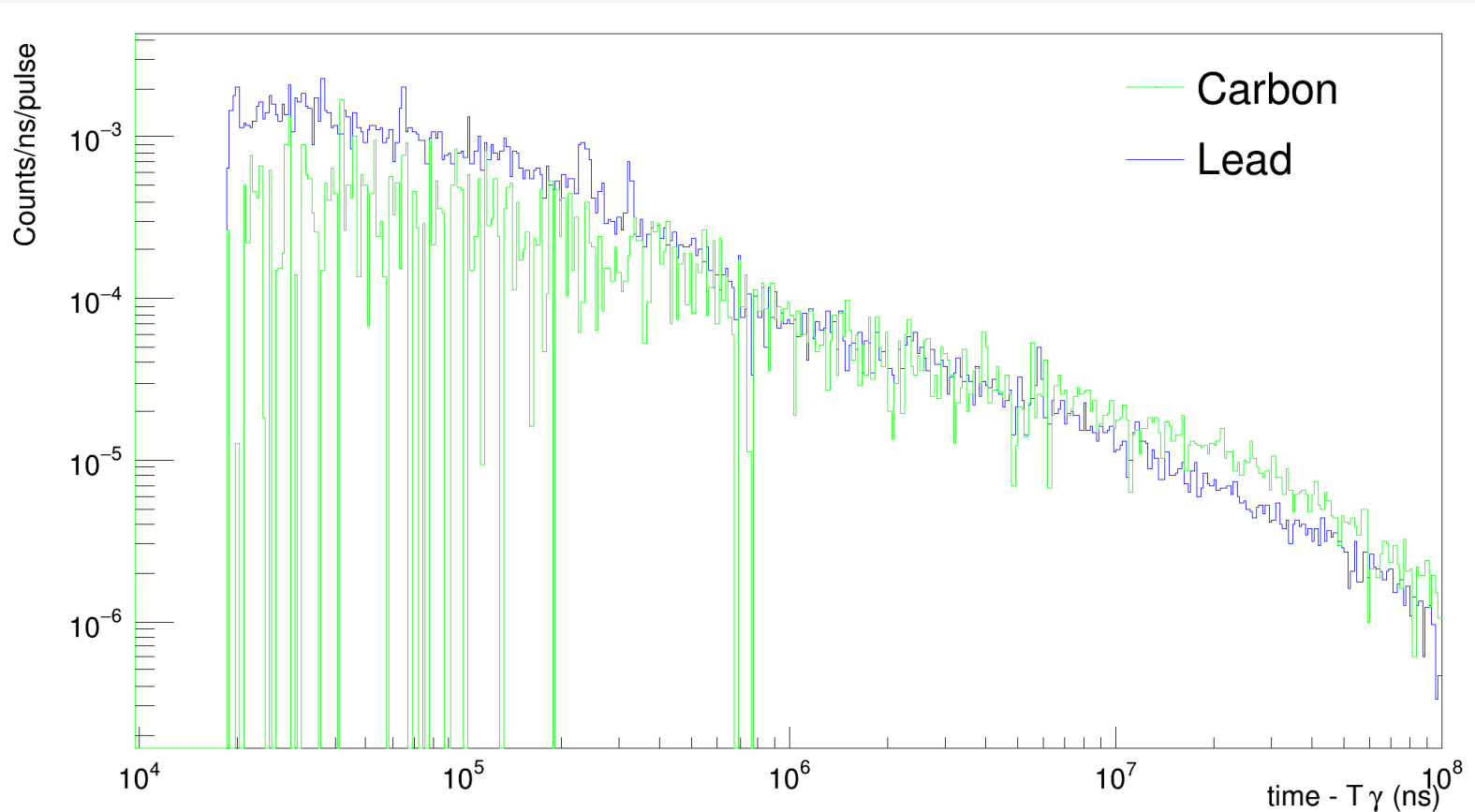
$b_n(t)$ and $b_\gamma(t)$ can be estimated via additional measurements with “perfect scattering” samples (materials with negligible capture cross-section), like lead and carbon.

Background measurements



- Set of measurements performed during the campaign
- Plotted in counts/ns to better understand the shape

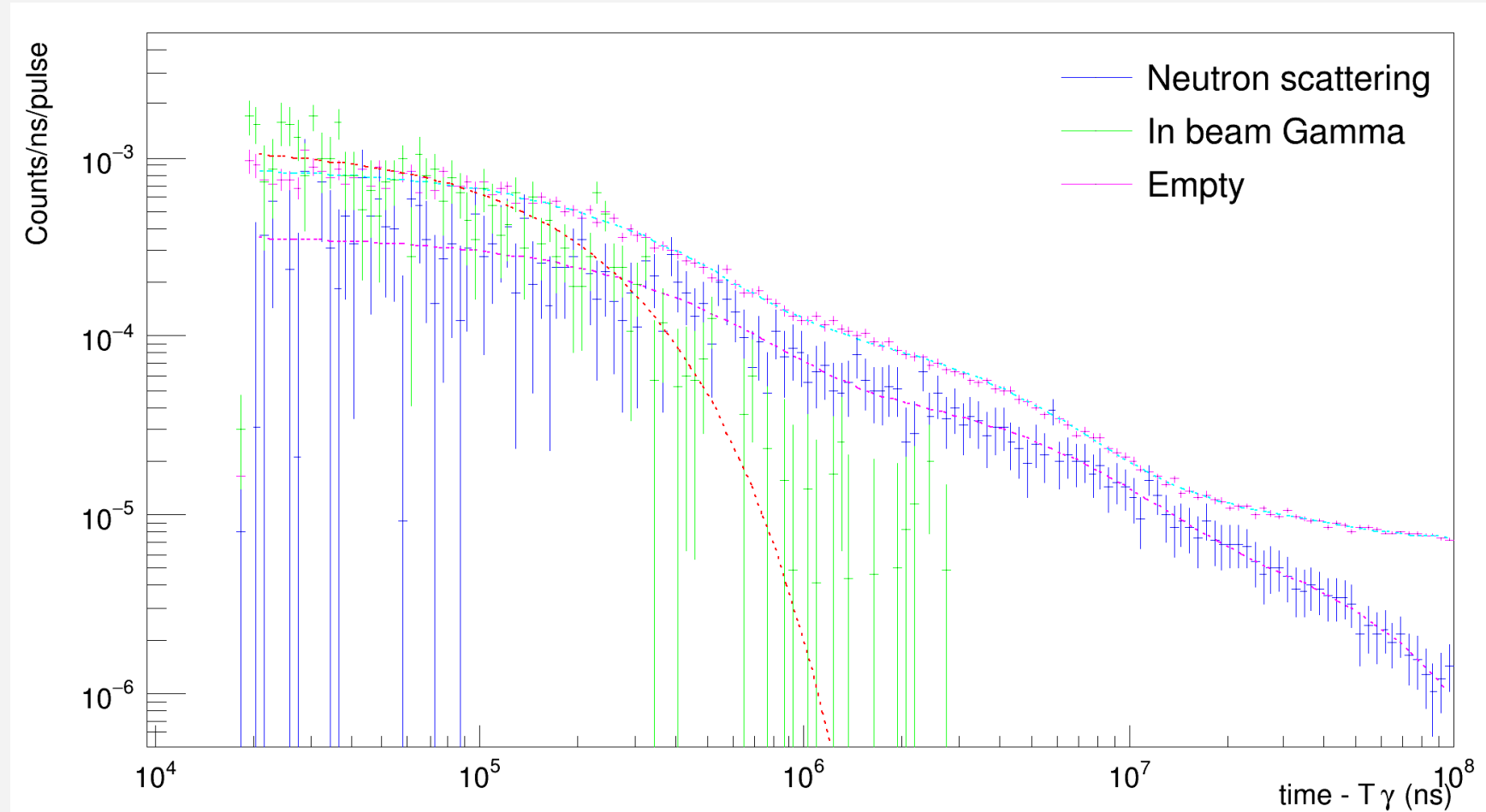
Neutron and gamma component estimation



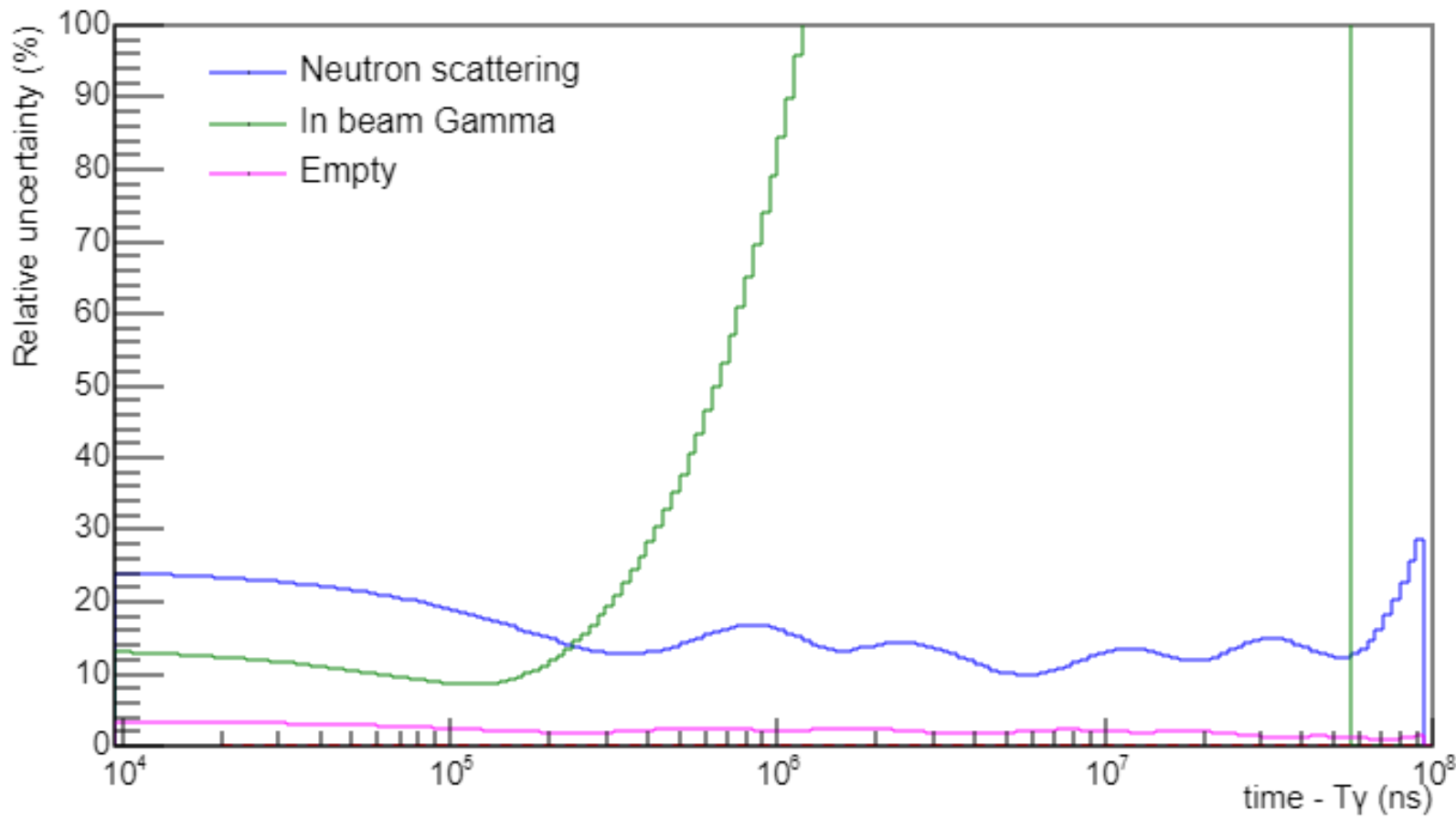
- Both lead and carbon sample are perfect neutron scatterers;
- Due to high Z, lead sample has a high gamma scattering cross-section;
- Empty counts removed from lead and carbon;
- Carbon spectra can be used to estimate neutron scattering component at higher energies;
- Carbon normalized to lead spectra below ~ 20 eV

Fit of background components

- Neutron scattering and in-beam gamma component fitted with analytical functions;
- Neutron component fitted with three exponentials;
- In-beam gamma fitted using exponential function;
- Fit functions can reproduce the experimental spectra.

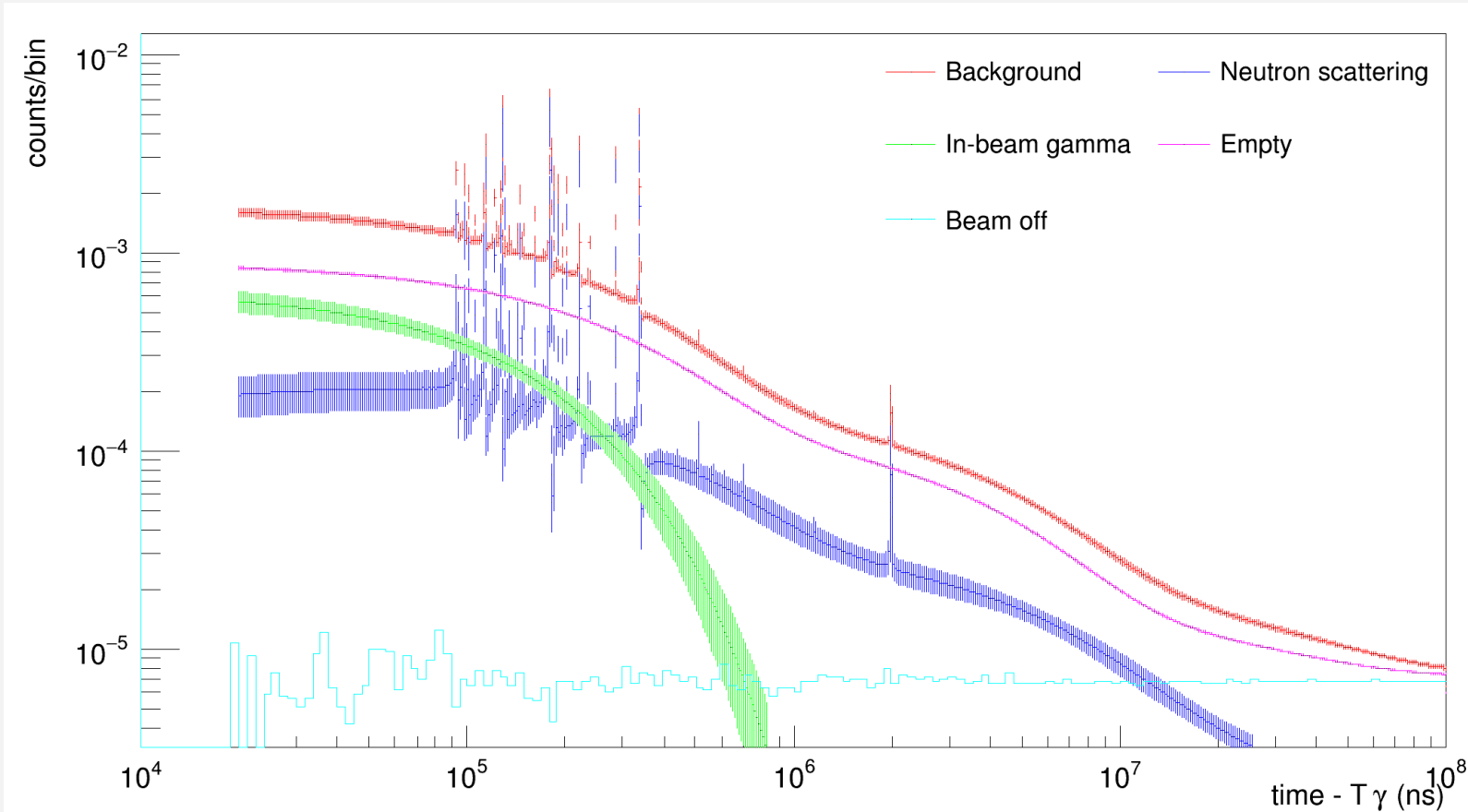


Background fit uncertainty



- Uncertainty on the fit estimated using 95% confidence interval extracted from Root.
- Almost constant uncertainty around 5% for Empty fit.
- Uncertainties around 15% for in-beam gamma at high energy and neutron scattering at low energies
- Fit uncertainty used as bin uncertainty in estimated background.

Total background



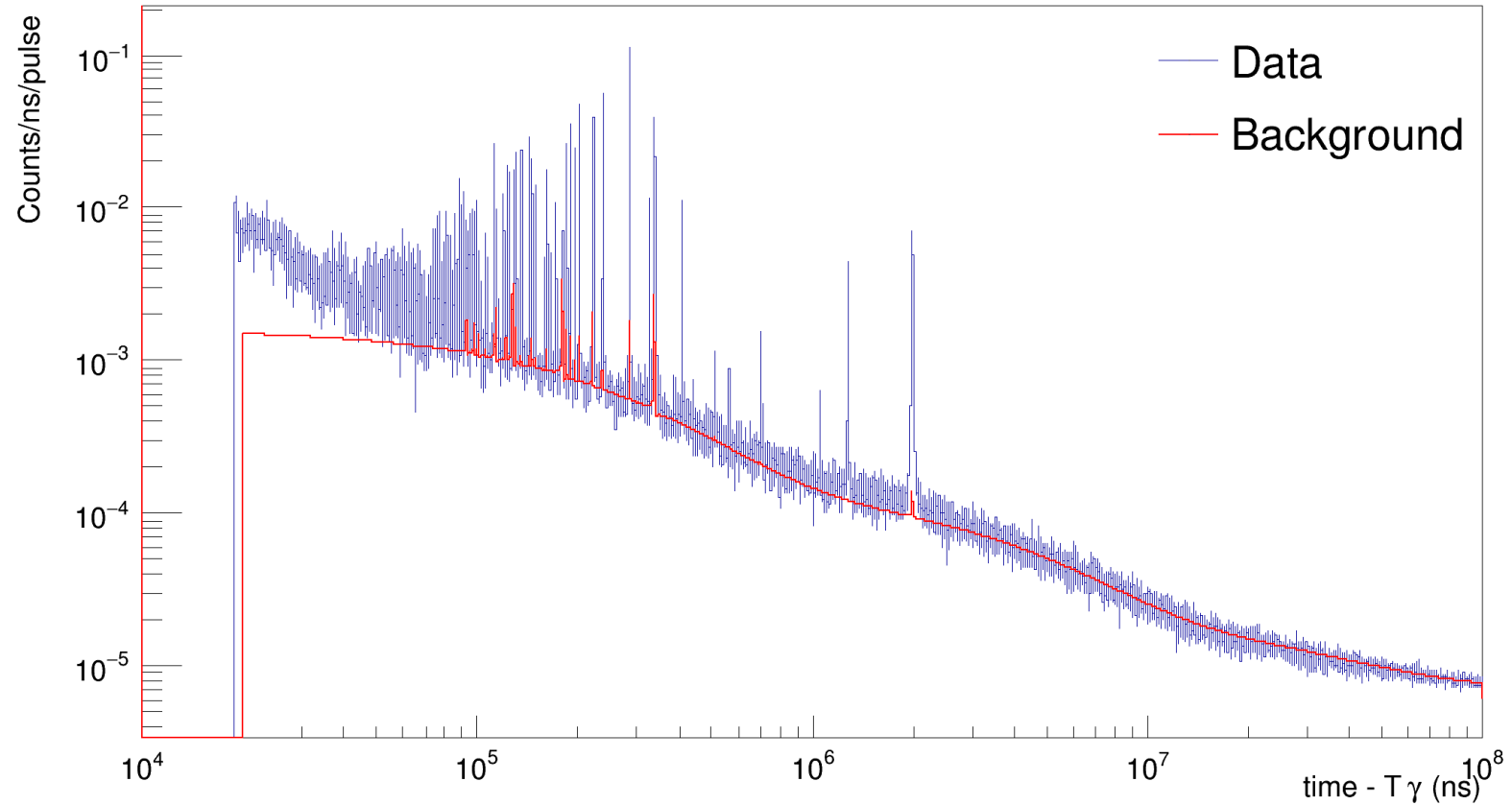
- Neutron scattering and in-beam gamma component scaled to reproduce effect of molybdenum samples:

$$B_n(Mo) = \frac{\sigma_{Mo}^{el}}{\sigma_{Pb}^{el}} \frac{n_{Mo}}{n_{Pb}} B_n(Pb)$$

$$B_\gamma(Mo) = \frac{Z_{Mo}}{Z_{Pb}} \frac{n_{Mo}}{n_{Pb}} B_\gamma(Pb)$$

- Different components added together to obtain total background of each sample.

Background subtraction



- Background subtracted from each sample count spectra.
- Quality of background estimated with gold sample measurements in both resolved and unresolved regions (see later).

Reaction yield

Reaction yield of capture measurements

For a capture experiment the observable of the measurement is the capture yield defined as:

$$Y_{exp} = N \frac{C_{\gamma}(t) - B_{\gamma}(t)}{\varphi(t)}$$

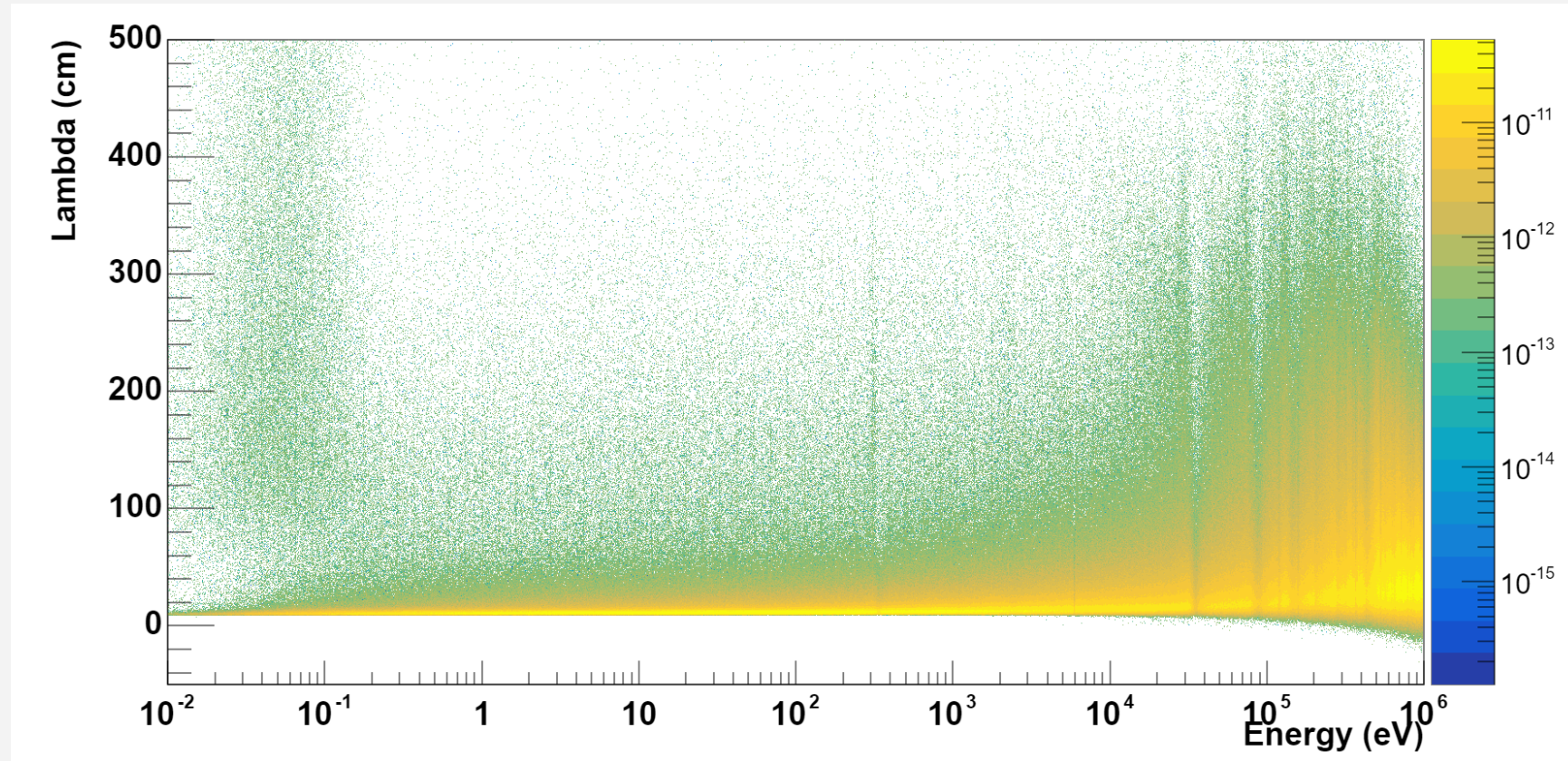
Where **N** is a normalization factor and $\varphi(t)$ is the neutron flux while at the numerator we have the experimental weighted counts and the background.

The normalization factor can be extracted from the saturated resonance of gold.

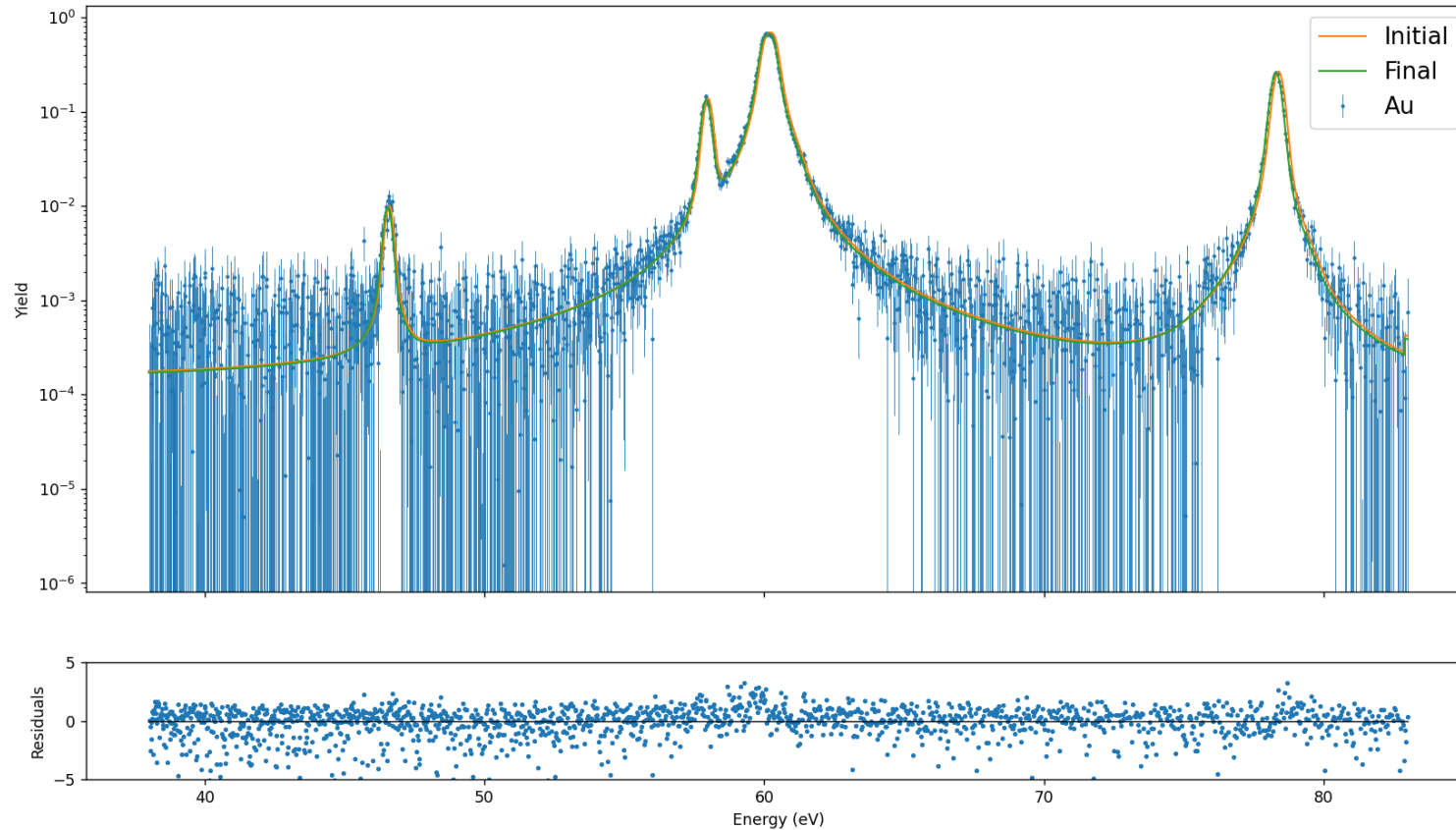
The neutron flux per proton pulse was evaluated during the commissioning.

Resolution Function

- The resolution function to be used in SAMMY was estimated using the Transport code;
- The flight-path to use was estimated by comparing the simulation with the gold spectra;
- The 2D histogram was converted in a SAMMY input using the RF2SAMMY code.



Time-to-Energy conversion

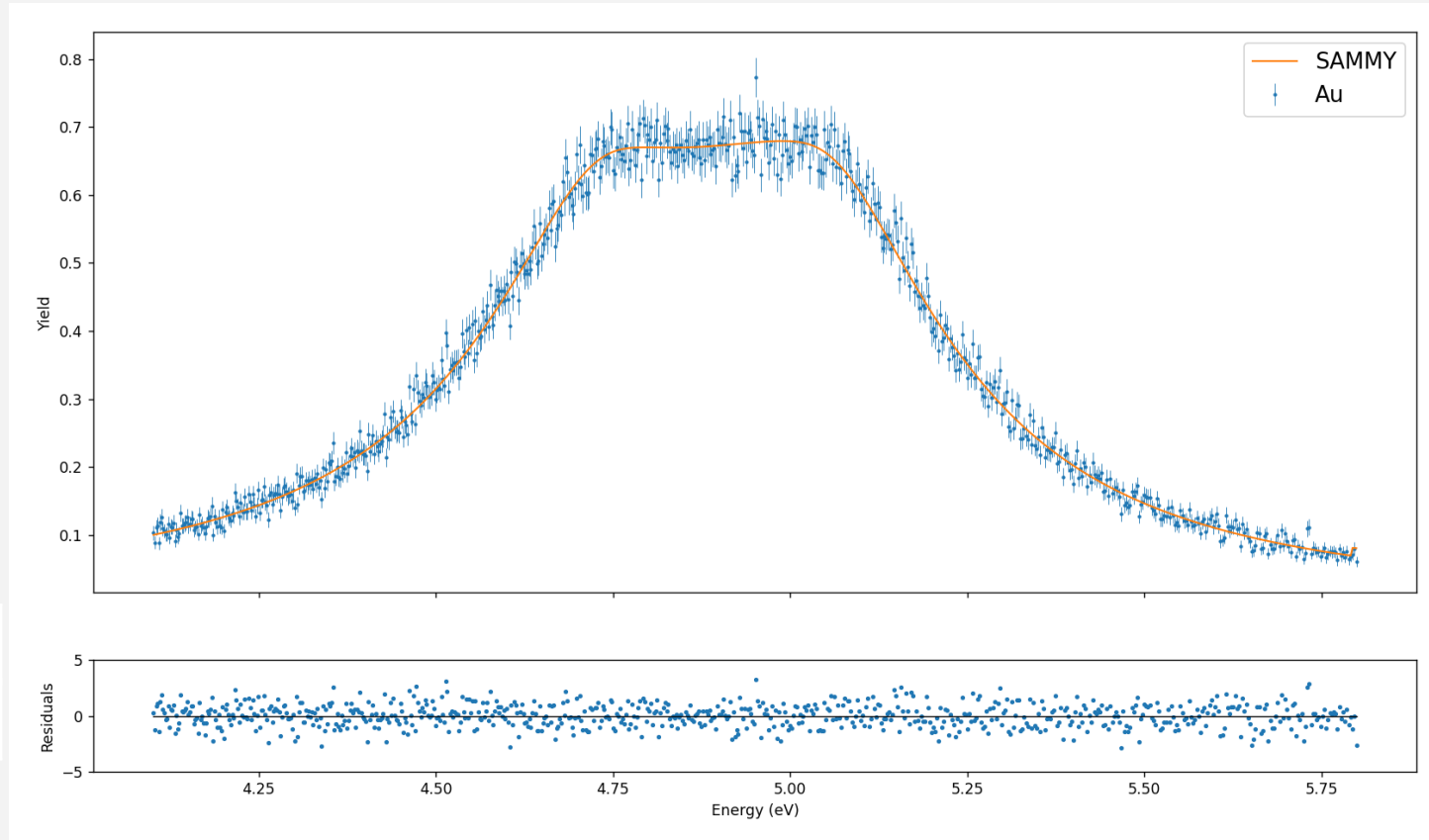


- To obtain the reaction yield as a function of energy an accurate knowledge of the flight-path length is needed.
- The flight-path length can be fitted using SAMMY and the first resonances of gold (<100 eV) to avoid effect of T0.
- Starting value of flight-path estimated using Transport Code

$L=183,9254 \text{ m}$

Normalization

- Normalization obtained from top flat region of saturated gold resonance at 4,9 eV.
- Normalization factor obtained for each detector individually.
- Normalization in agreement within 3%

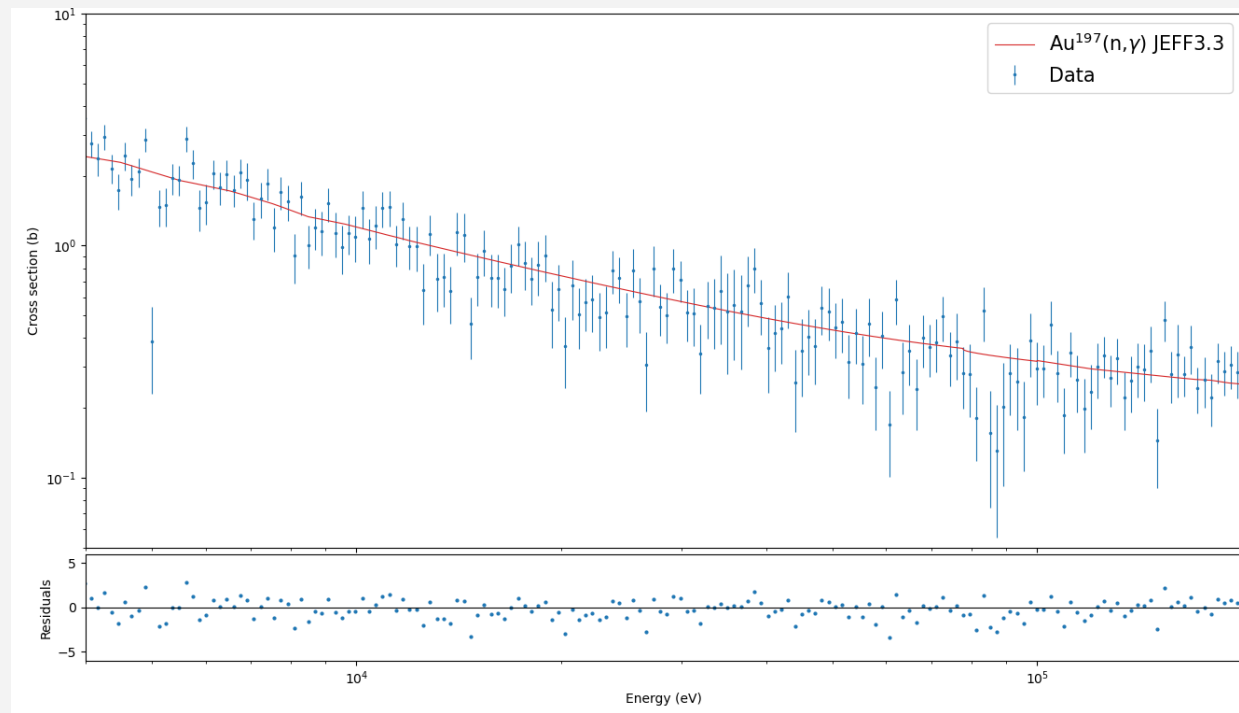
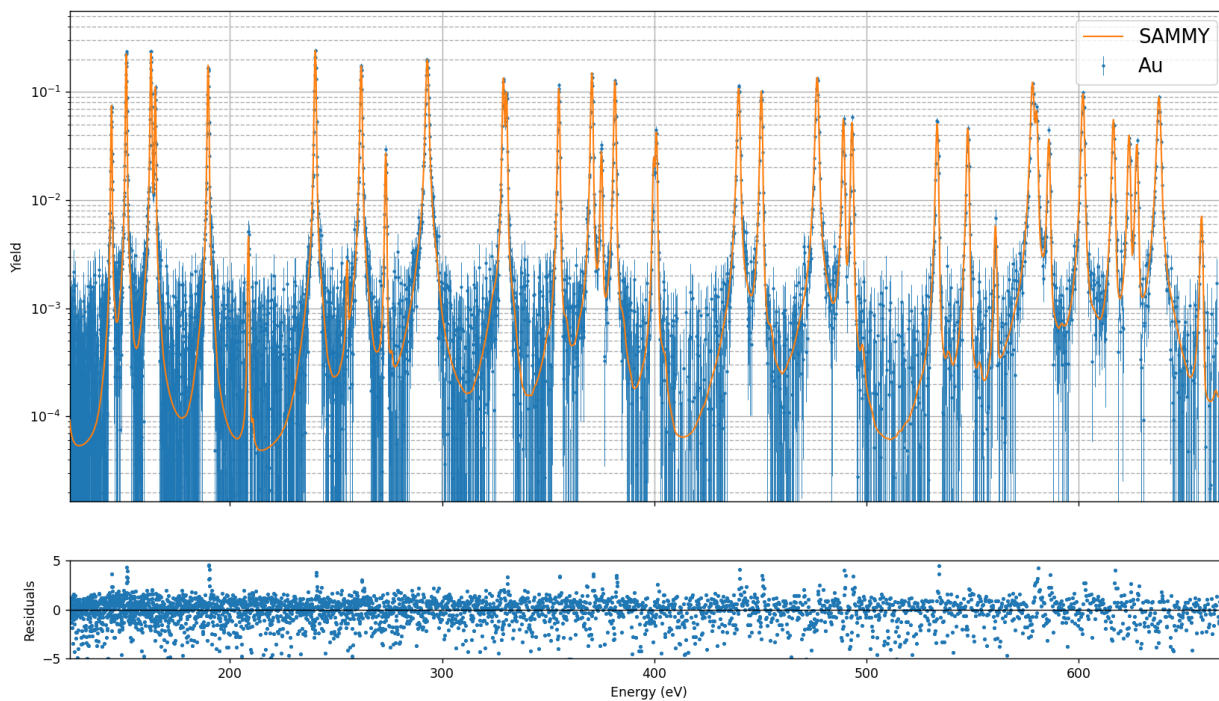


C6D6 1	C6D6 2	C6D6 3	C6D6 4
0,710056	0,701284	0,71994	0,688226

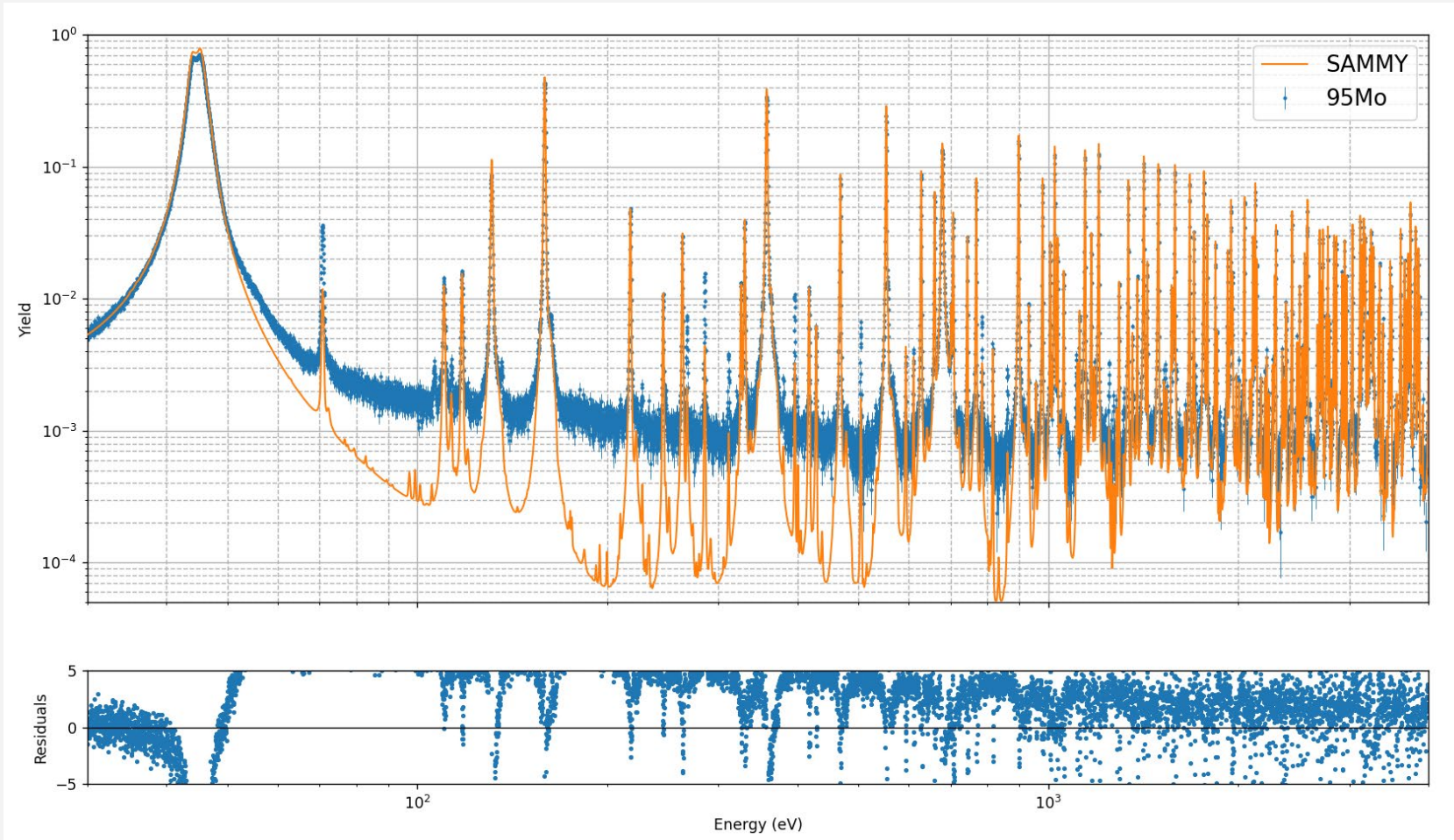
Comparison of Au spectra with literature

The reaction yield obtained with the gold sample was compared with the literature values for the resolved and unresolved resonance region.

The good agreement of our spectra with the literature validate the correctness of the procedure used.

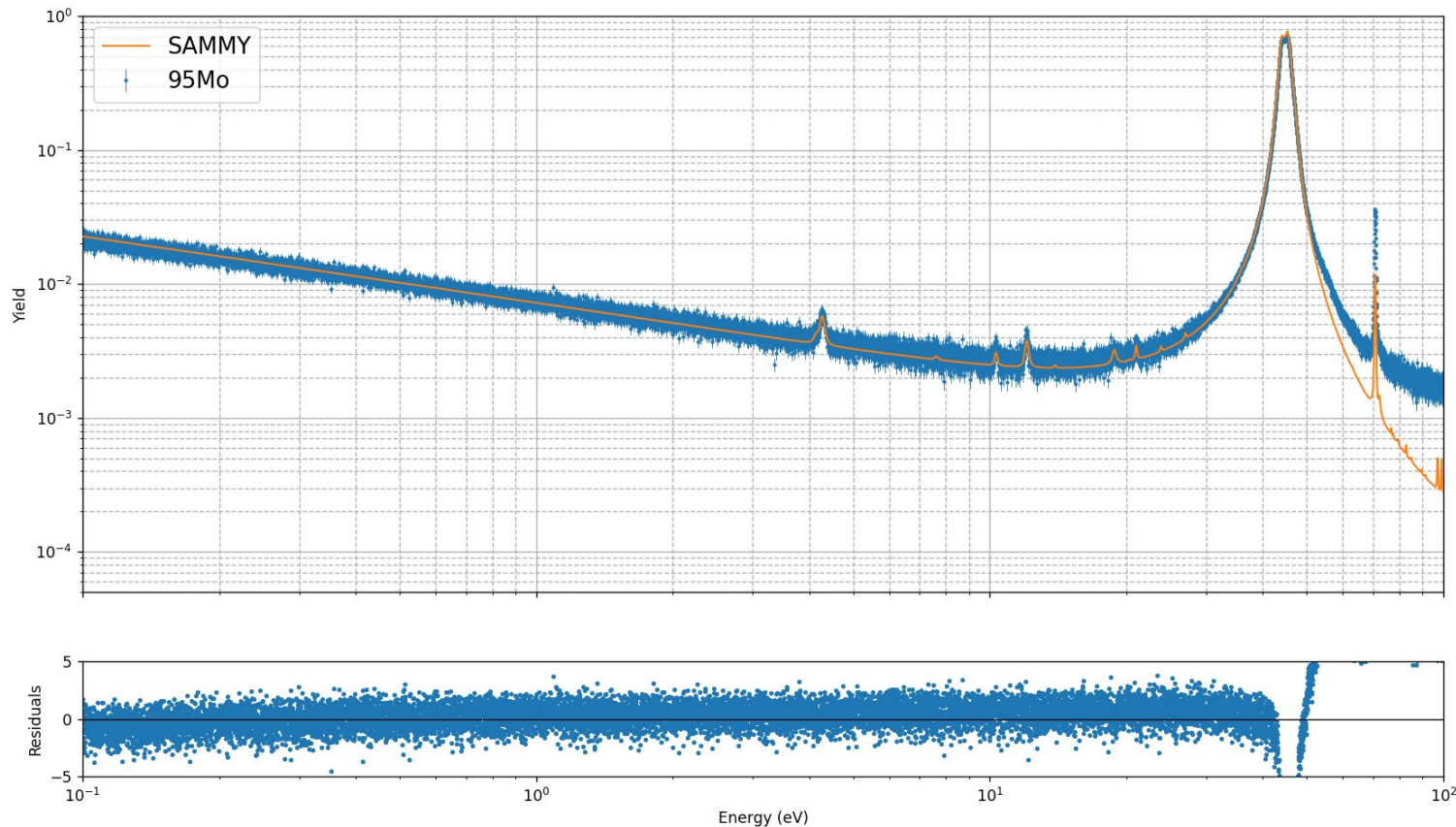


Background Mo samples - RRR



- Comparison of measured yield with calculation of SAMMY for ⁹⁵Mo;
- Background level higher than expected between 50 eV and ~5 keV;
- Same effect, with smaller magnitude, visible in ⁹⁶Mo;
- ⁹⁴Mo sample seems almost unaffected;
- Investigation on possible causes still ongoing.

Background Mo samples - Thermal



- Comparison of measured yield with calculation of SAMMY for ^{95}Mo at thermal energies;
- Good agreement down to $\sim 200\text{meV}$
- Effect of small contaminants ($\sim 1\text{E-}4$) of W and Ta visible at low energies
- Same good agreement can be seen in $^{94,96}\text{Mo}$

Preliminary resonance fit

Simultaneous fit with SAMMY

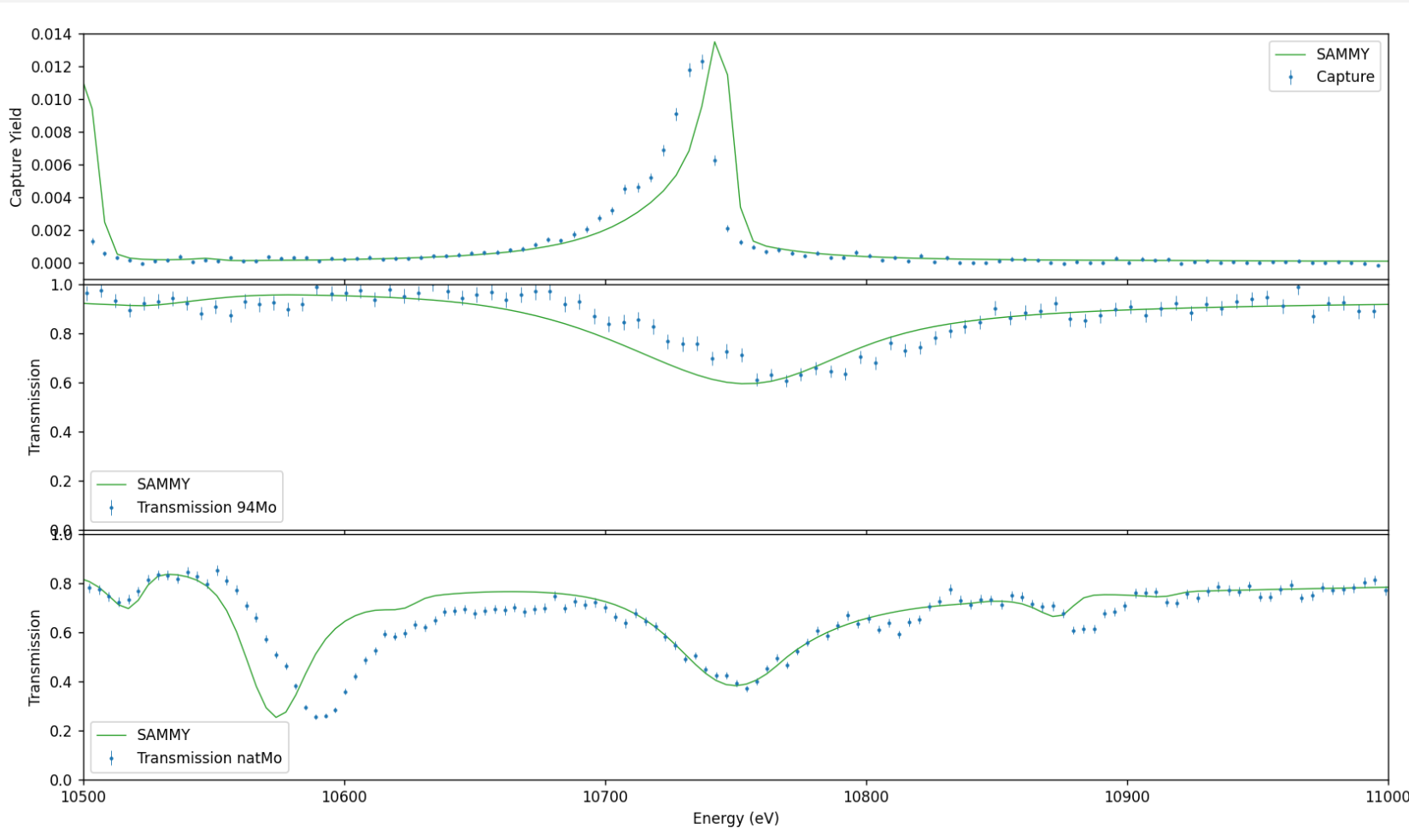
Resonance parameters for ^{94}Mo can be obtained using **SAMMY** by fitting capture data in parallel with transmission data with enriched and natural samples obtained at GELINA.

The resolution function of GELINA has been converted from the REFIT format and added to SAMMY.

The resonance parameters used as starting point are the ones obtained from literature and corrected with transmission at 50m with $^{\text{nat}}\text{Mo}$ samples.

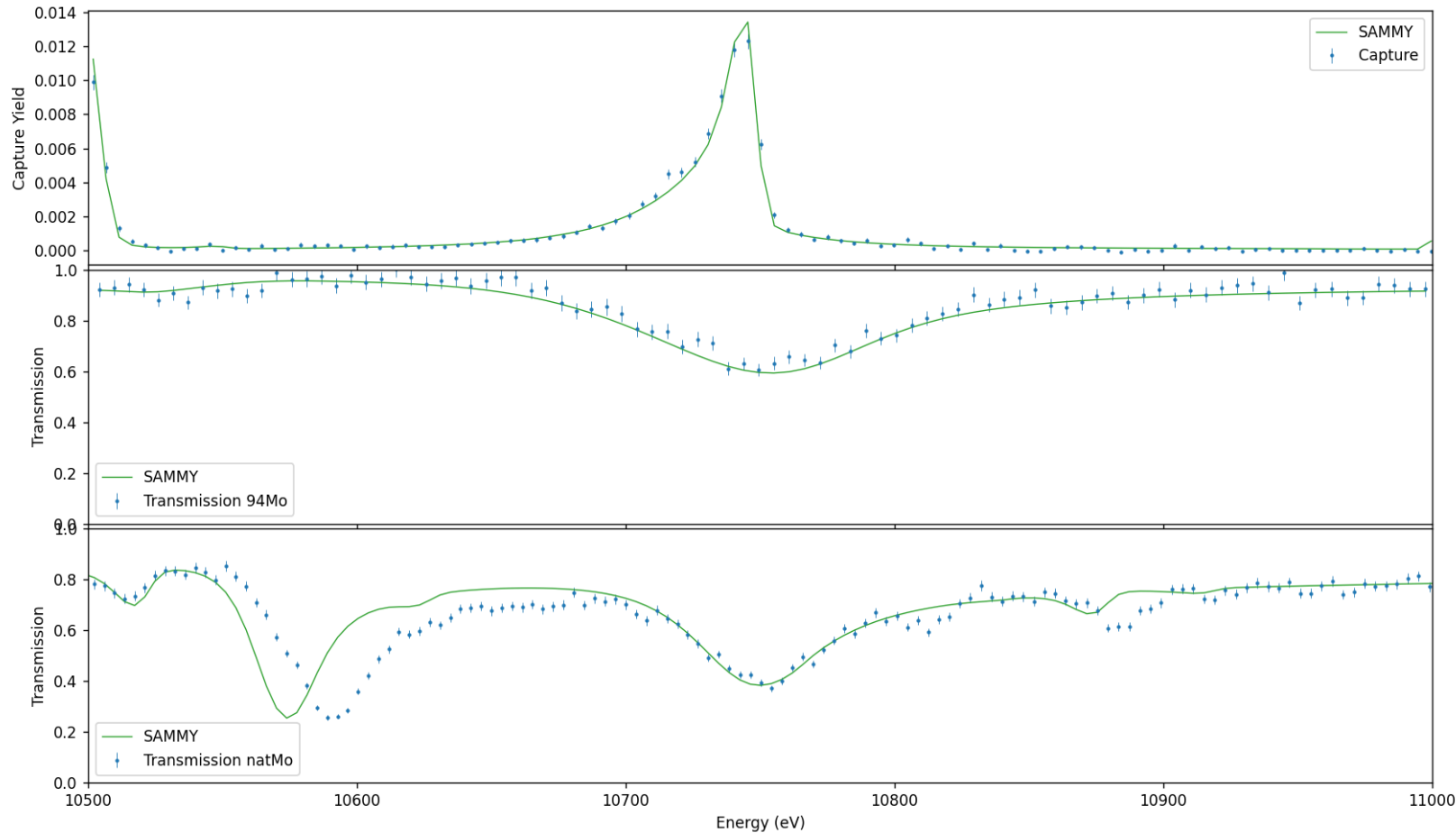
The parameters above 5keV were taken from **JENDL5**. A bound level was added to all the isotopes (except ^{96}Mo) to reproduce the thermal cross-section of **JEFF4**.

Preliminary adjustments - T0 correction



- A disagreement between the resonance energies obtained with capture and transmission data was observed.
- The disagreement is present also between transmission data at 10 and 50m.
- To better match the energies between the different datasets a T0 was applied to the n_TOF and 10m transmission data using the transmission at 50m as a reference.

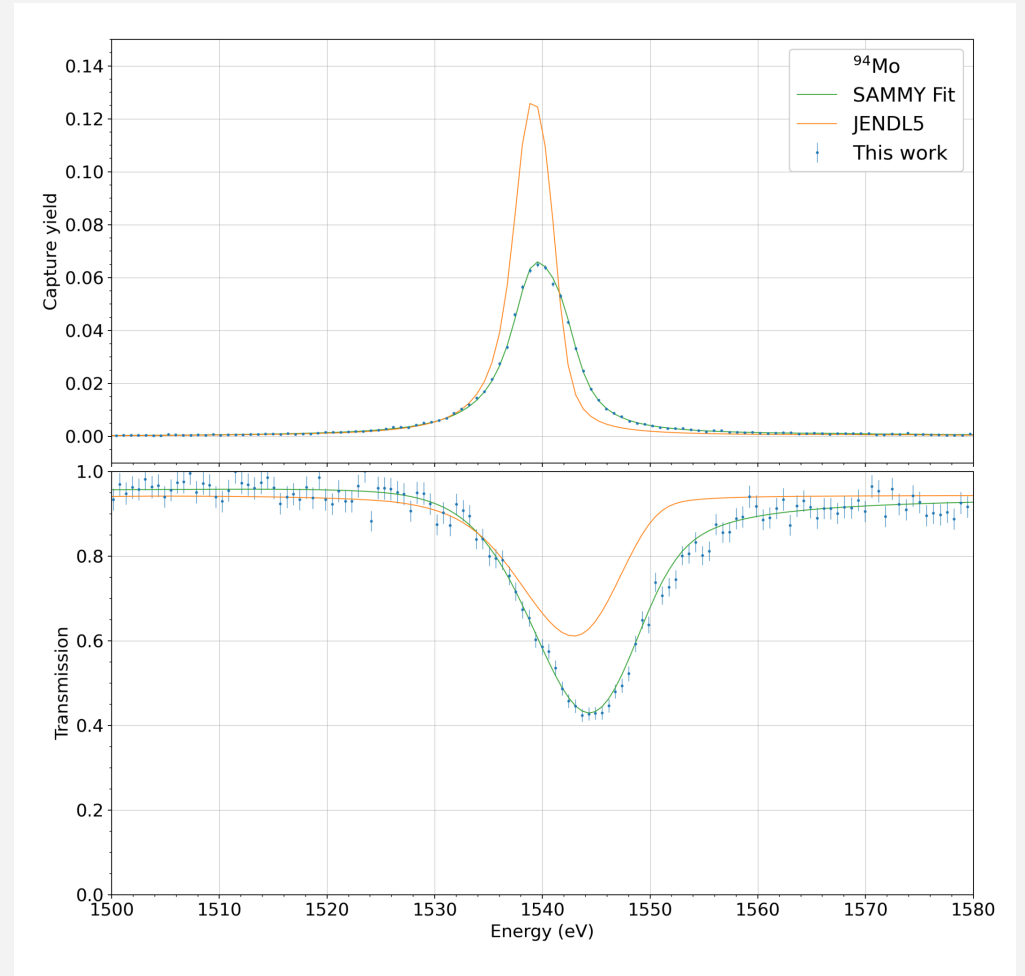
Preliminary adjustments - T0 correction



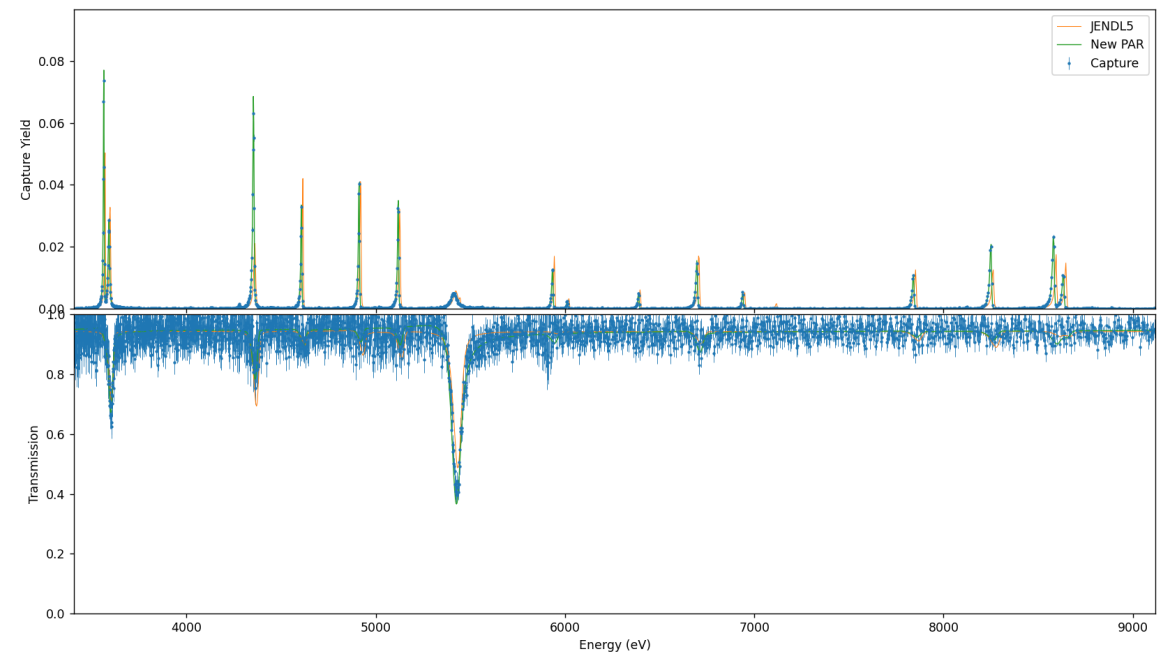
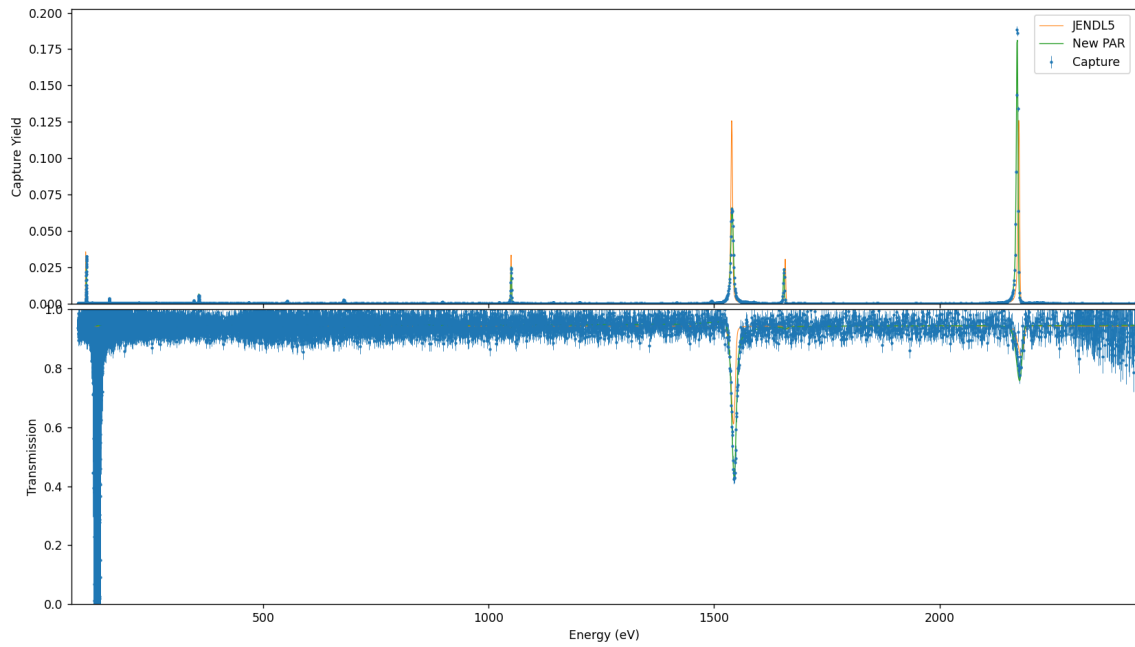
- The T0 was fitted using many different isolated resonances of different Mo isotopes.
- The resonance energy of the 50m transmission was further adjusted above 5keV.
- An average value of T0 was obtained from the different resonances.
- A value of **50ns** and **-7ns** was obtained for n_TOF and 10m transmission, respectively.
- With this correction a good agreement between the different dataset can be observed in all the energy range

Preliminary resonance parameters ^{94}Mo

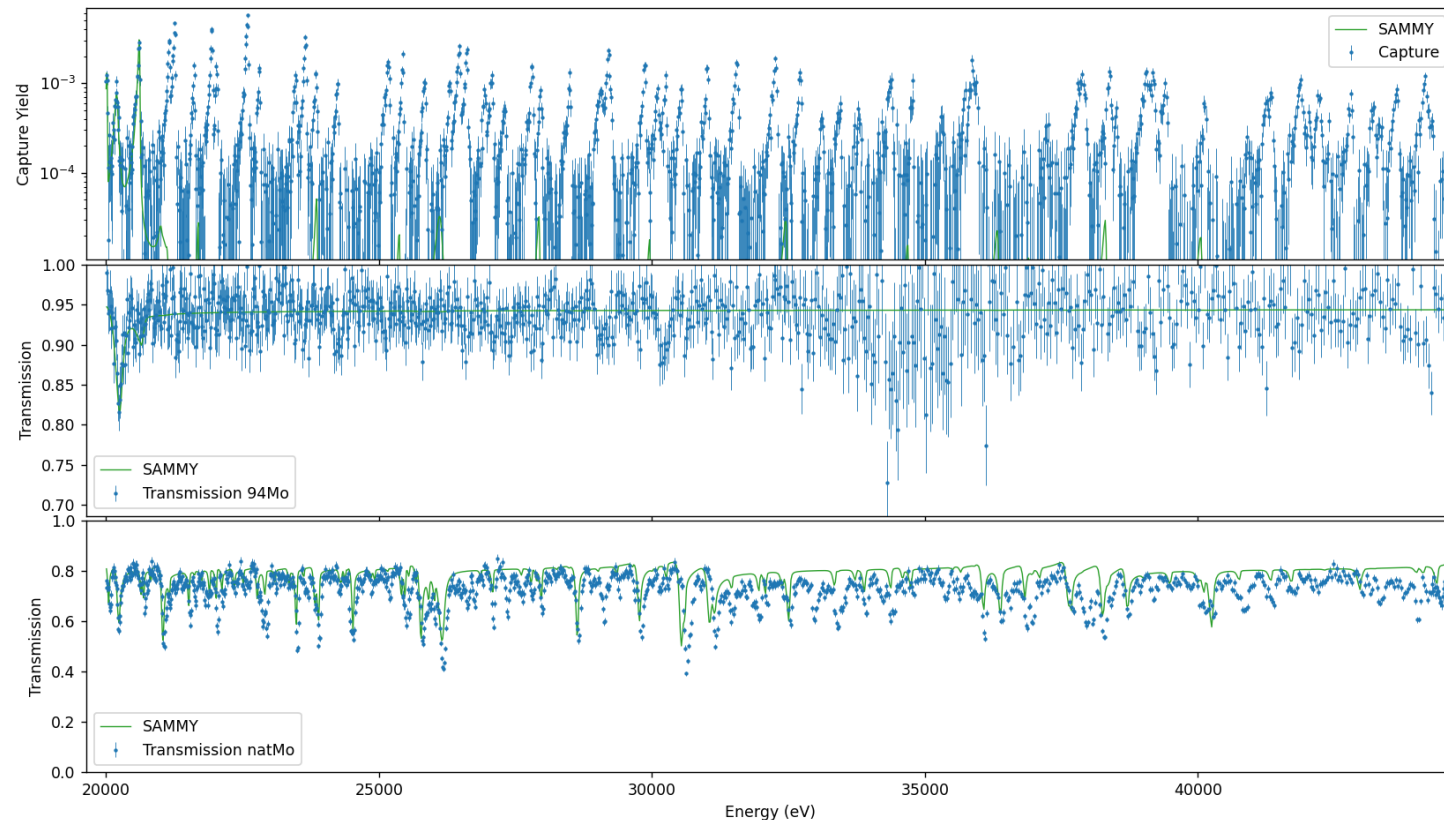
- Resonance parameters have been adjusted in all the resolved resonance region (<21 keV);
- Example of fit showed here compared to the calculation performed with JENDL5 parameters
- Good agreement between transmission and capture data with enriched samples



Preliminary resonance parameters ^{94}Mo

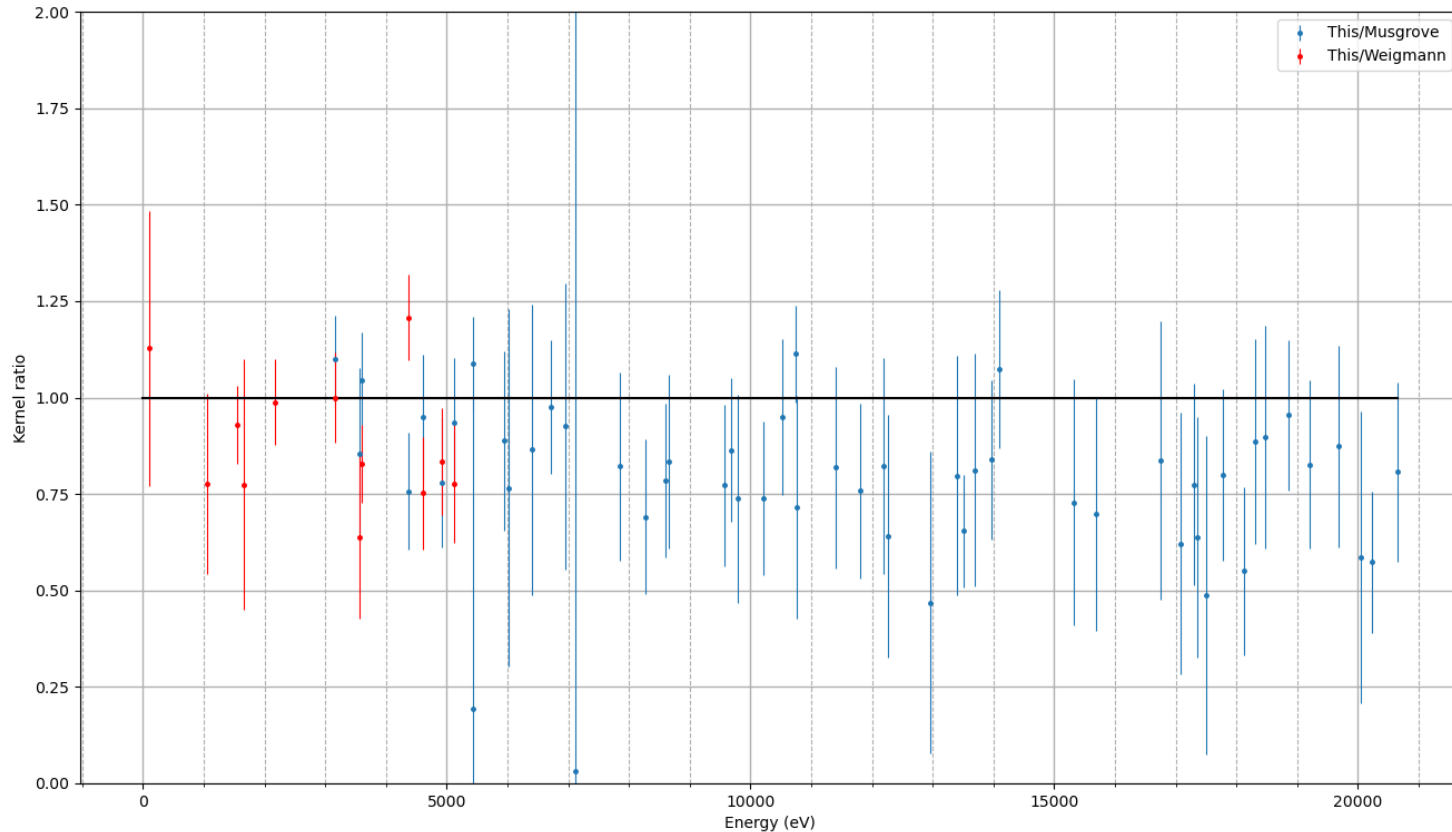


Extending resolved resonance region



- Resolved resonance region in JENDL5 stops at ~ 20 keV;
- Using n_TOF data is possible to extend the RRR at higher energies;
- Few resonances visible also in transmission measurement;
- The RRR could be extended up to ~ 50 keV.

Kernel ratio with literature



- The preliminary kernels obtained with SAMMY were compared to the ones in literature (Weigmann and Musgrove capture measurements);
- Systematic deviation of around 20% observed
- Possible causes still under investigation

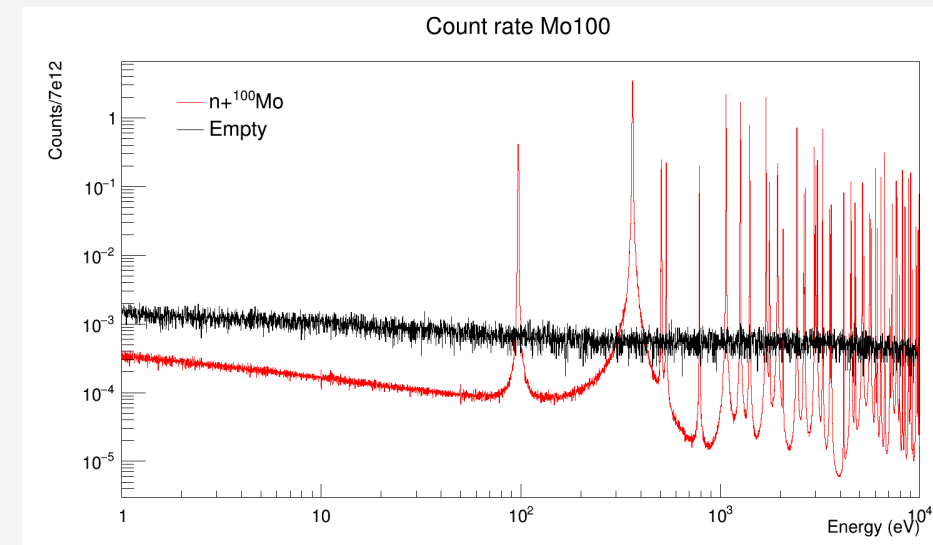
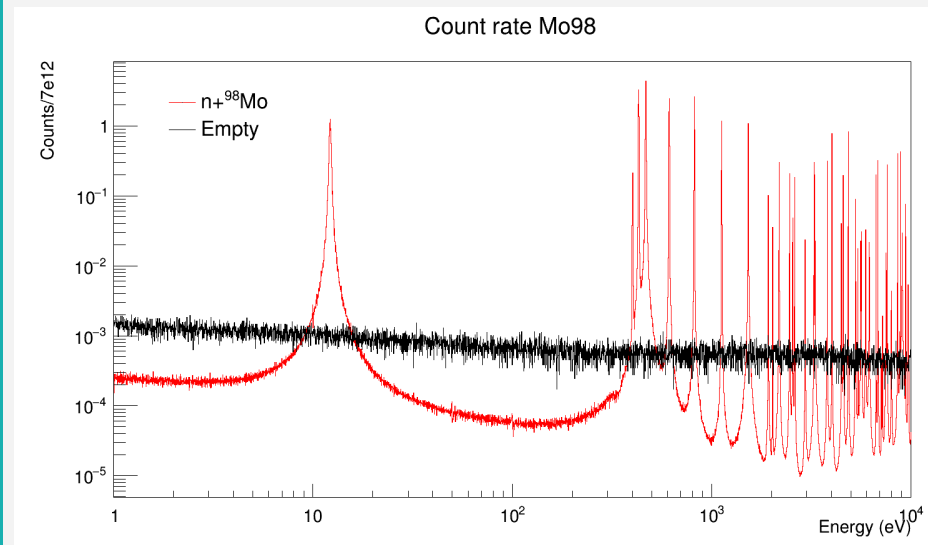
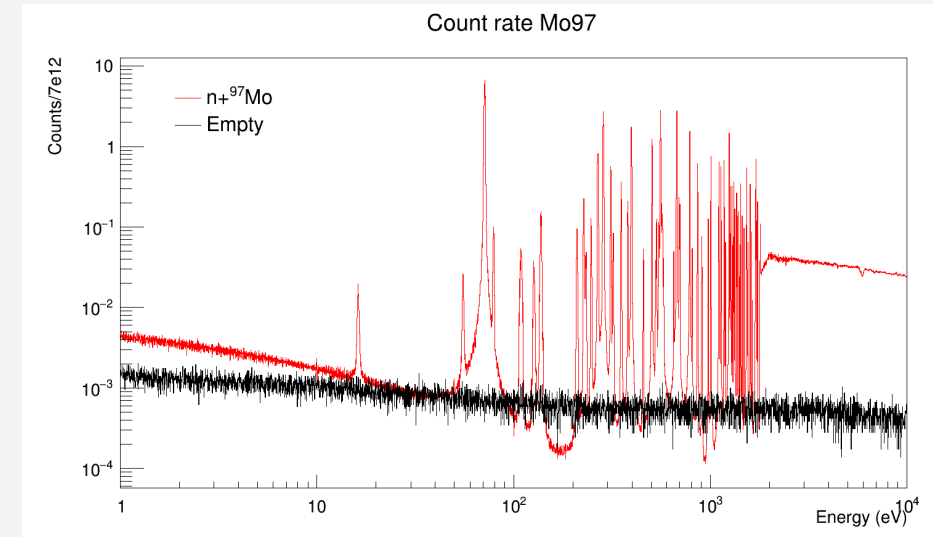
Possible proposal of new Mo isotopes measurements

Overall	
Rank	isotope
5	92
1	94
4	95
2	96
3	97
6	98
7	100

- Ranking of interest of different Mo isotopes based on the role in astrophysics, nuclear technology and cross-section uncertainties in literature,
- Three isotopes already measured,
- ^{92}Mo has low priority for astrophysics (p-only isotope),
- Possible addendum to measure $^{97,98,100}\text{Mo}$ to be prepared for next INTC.

Count rate estimate

- Count rate estimate for 2g samples in EAR1
- Empty measured during Mo campaign,
- New evaluated flux used in estimation



Summary and outlook

What has been done:

- Full background estimation and subtraction for all the detectors;
- Reaction yield calculation;
- Preliminary resonance analysis of ^{94}Mo using capture and transmission data simultaneously.

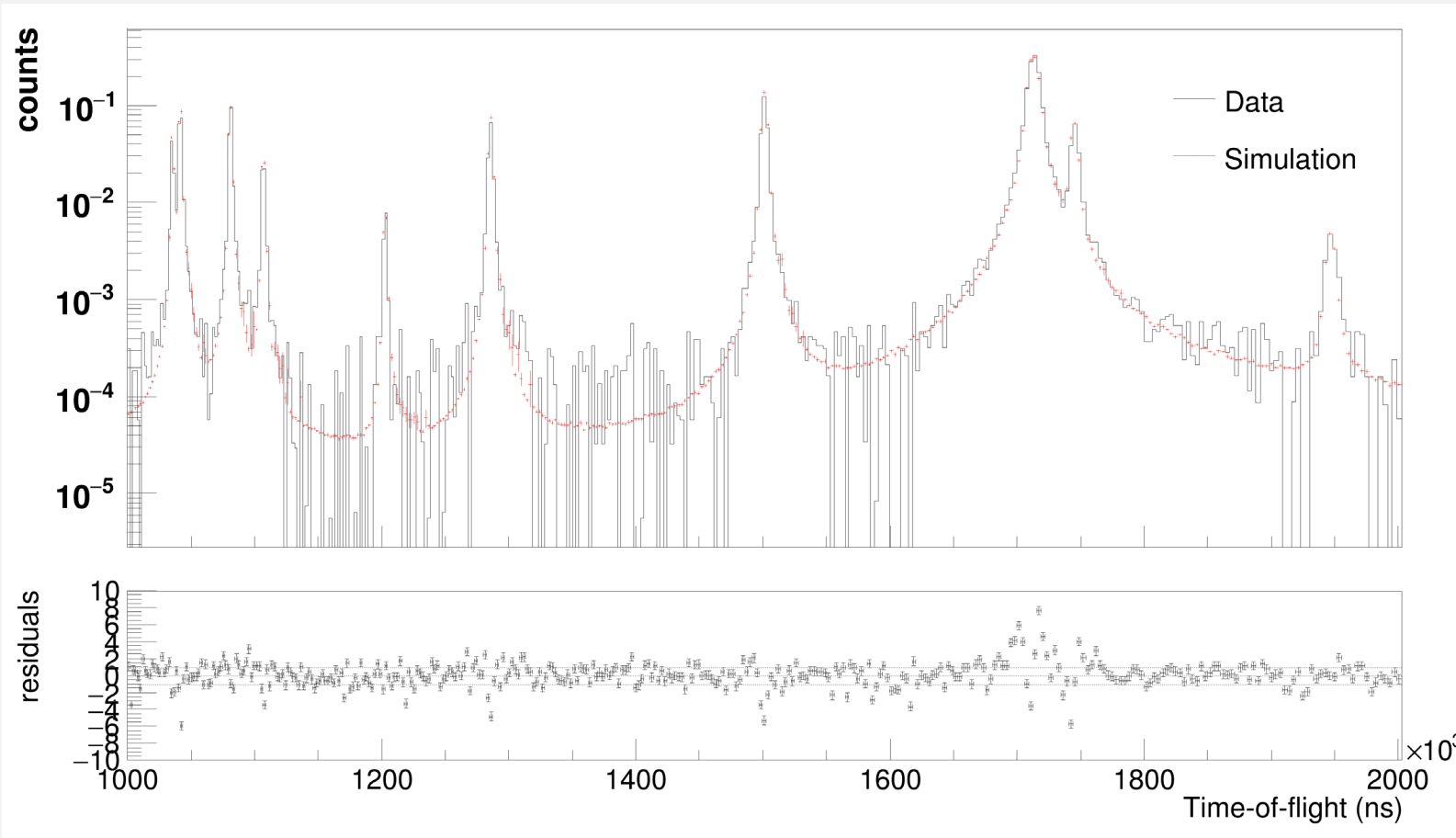
What is left to do:

- Correction of additional background in Mo samples;
- Final resonance analysis of $^{94,95,96}\text{Mo}$;
- Analysis of EAR2 data of 2022;
- R-Matrix analysis together with EAR2 data.

Thank you for your attention

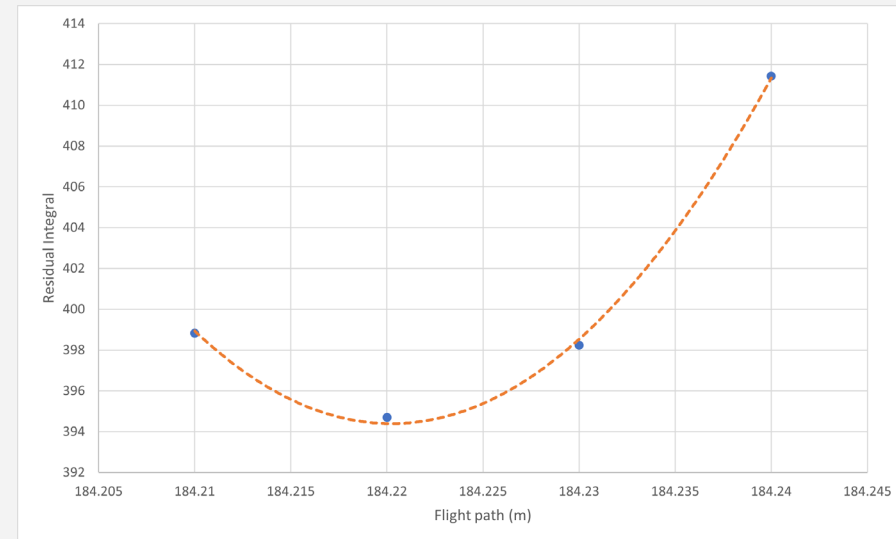
Backup

Transport code Flight-path



- Comparison of time-of-flight spectra measured with gold and the one obtained with the Transport code;
- Best flight-path was found by minimizing the residuals at different L_{TC} .

$$L_{TC} = 184,22 \text{ m}$$



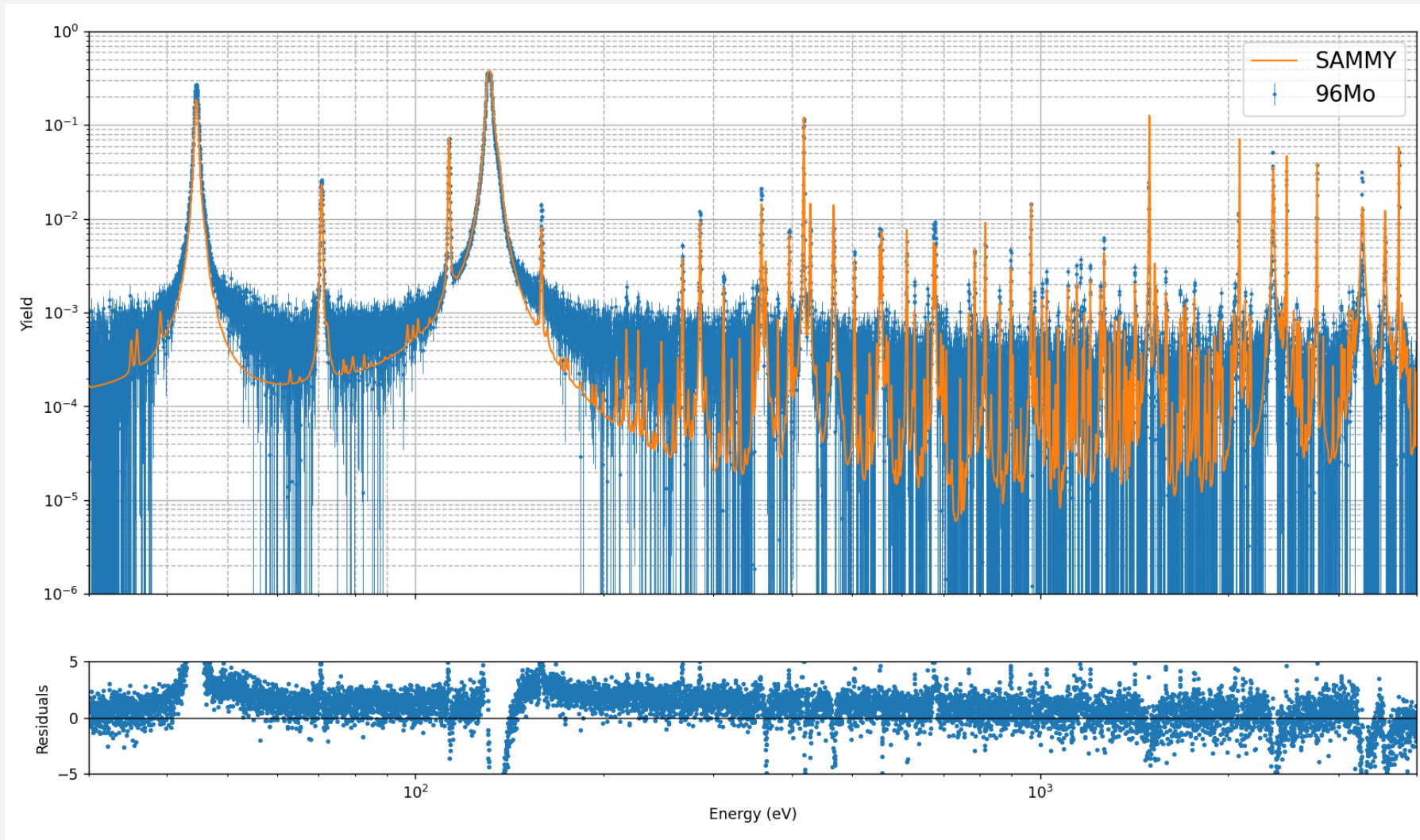
T0 resonance fit

⁹⁴ Mo	T0 fit
1542	0.0578
2176	0.1452
4360	0.0360
5433	0.0575
10757	0.0505
13515	0.0588

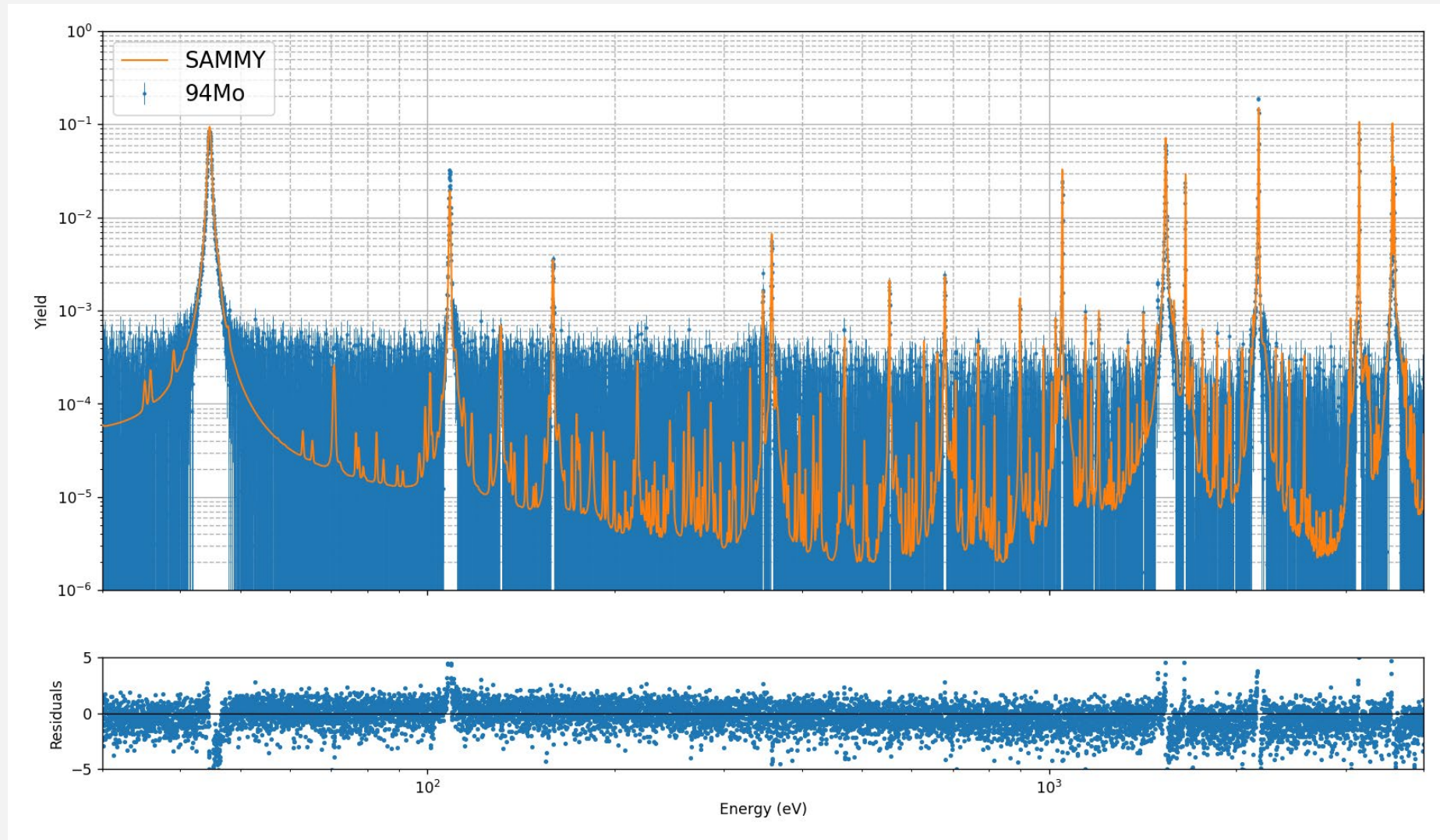
⁹⁵ Mo	T0 fit
1203	0.0604
1767	0.0305
3623	0.0368
3723	0.0375
4030	0.0407

⁹⁶ Mo	T0 fit
3571	0.0557
3756	0.0070
4320	0.0740
5384	0.0337
9393	-0.0171
10000	0.0420

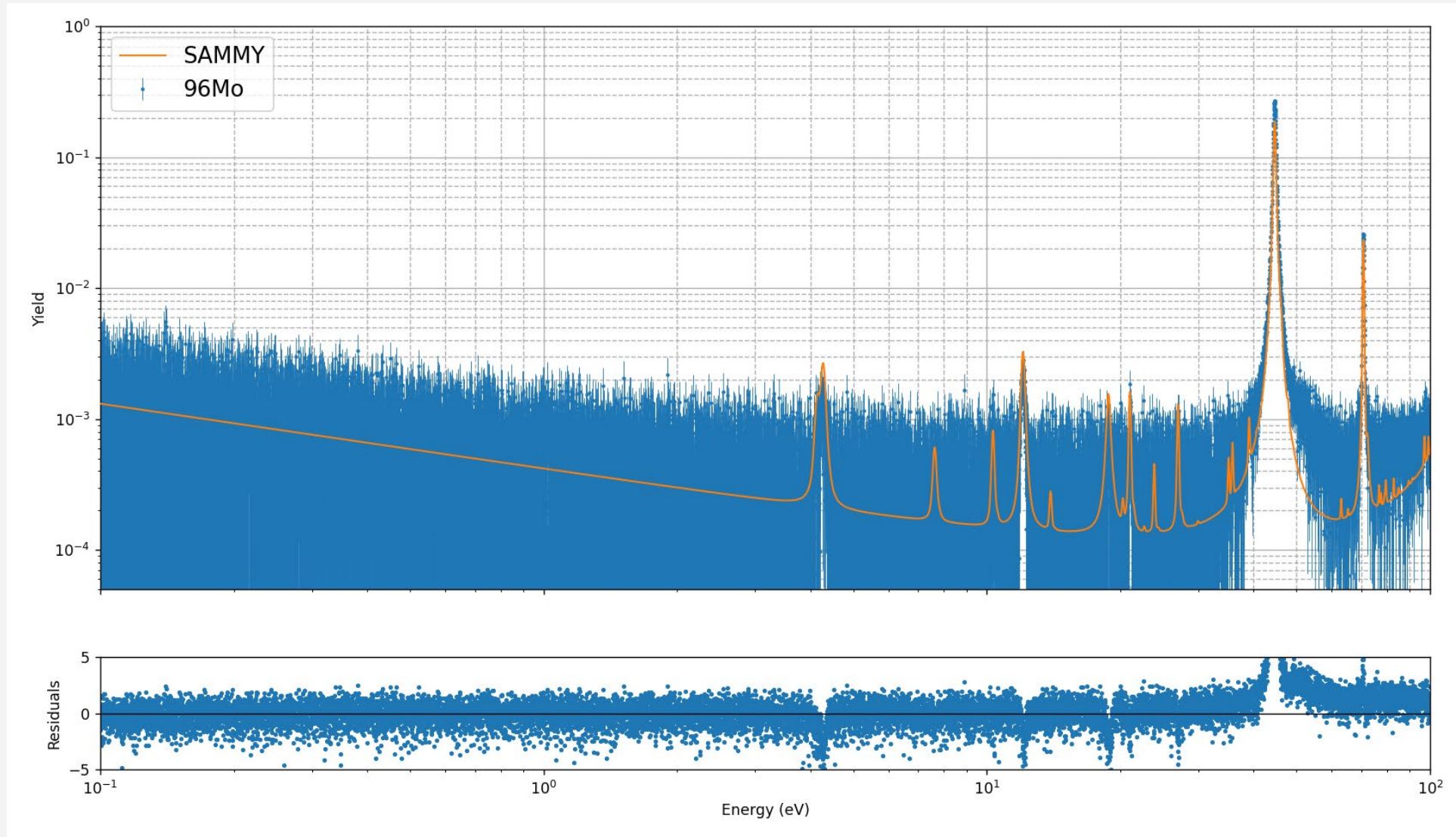
Background Mo samples - 96Mo



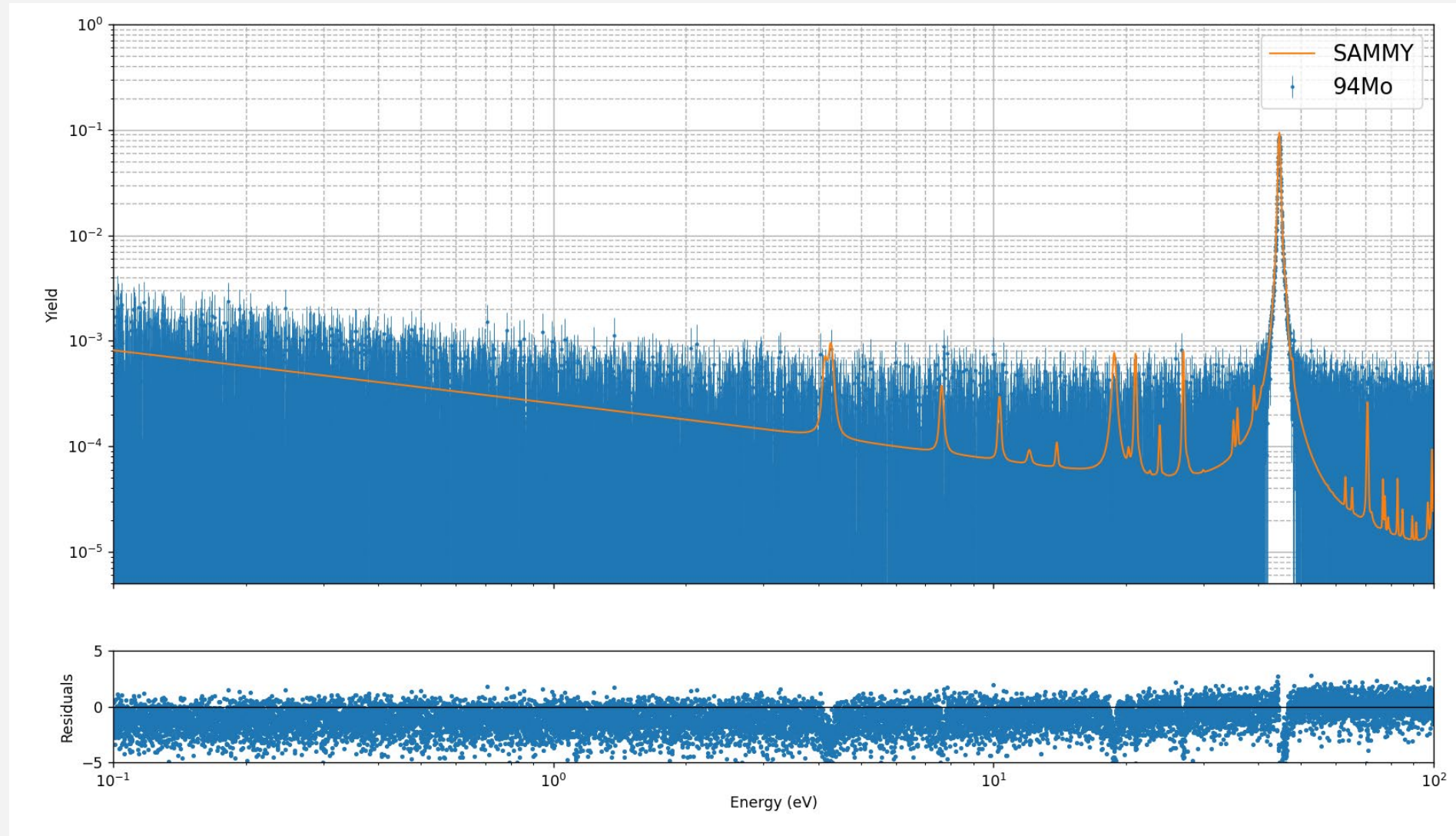
Background Mo samples - ^{94}Mo



Background Mo samples - 96Mo



Background Mo samples - ^{94}Mo



Mo pellet samples

Atomic %	⁹² Mo	⁹⁴ Mo	⁹⁵ Mo	⁹⁶ Mo	⁹⁷ Mo	⁹⁸ Mo	¹⁰⁰ Mo
⁹⁴ Mo	0,63%	98,97%	0,36%	0,01%	0,01%	0,01%	0,01%
⁹⁵ Mo	0,31%	0,69%	95,40%	2,24%	0,51%	0,65%	0,20%
⁹⁶ Mo	0,28%	0,24%	1,01%	95,90%	1,00%	1,32%	0,25%

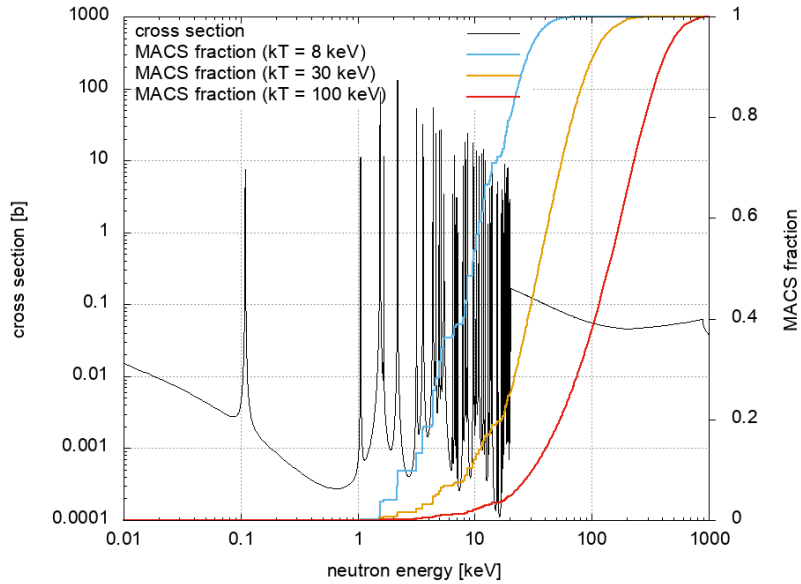
Isotope	Mass (g)	Areal density (atoms/b)
⁹⁴ Mo	1,9526	3,9592E-03
⁹⁵ Mo	1,9745	3,9558E-03
⁹⁶ Mo	1,9175	3,8064E-03
natMo-5 μm	2,014	4,0059E-03
natMo-350 μm	1,989	3,9584E-03

natMo abundances

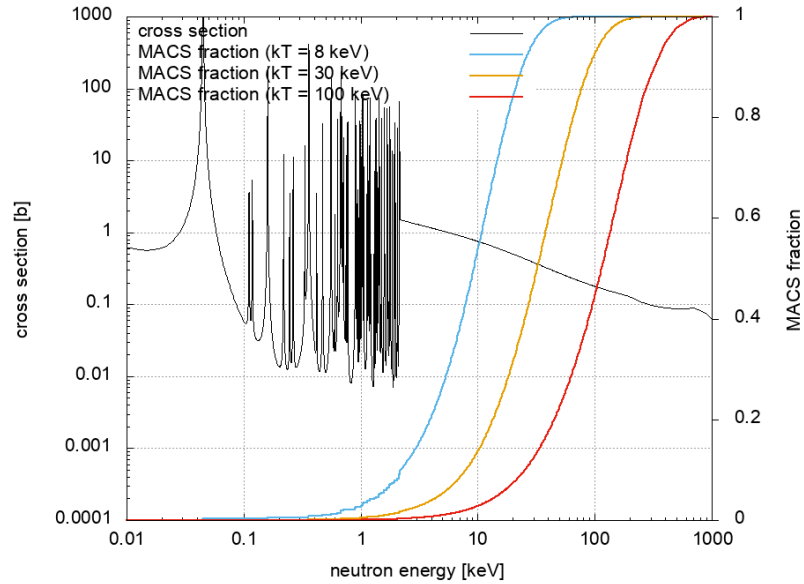
Isotope	Abundance
^{92}Mo	14.84%
^{94}Mo	9.25%
^{95}Mo	15.92%
^{96}Mo	16.68%
^{97}Mo	9.55%
^{98}Mo	24.13%
^{100}Mo	9.63%

MACS fractions

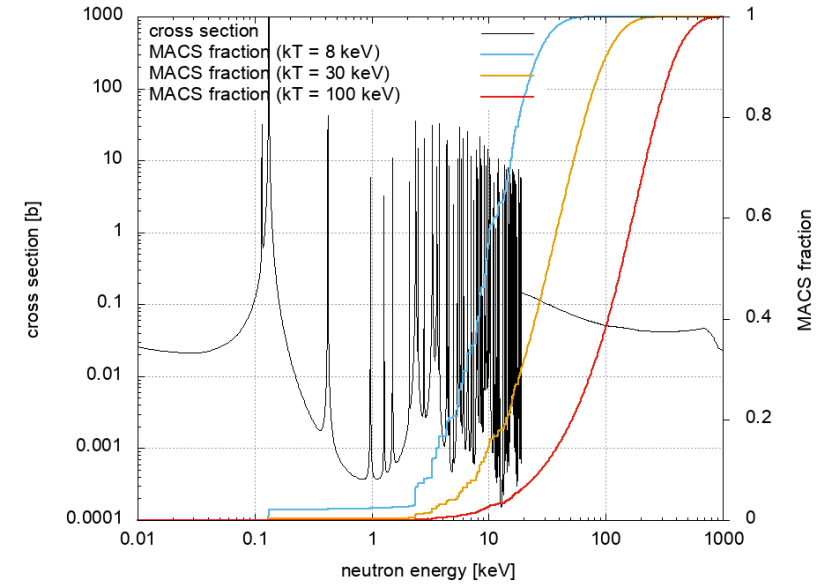
Mo-94



Mo-95



Mo-96



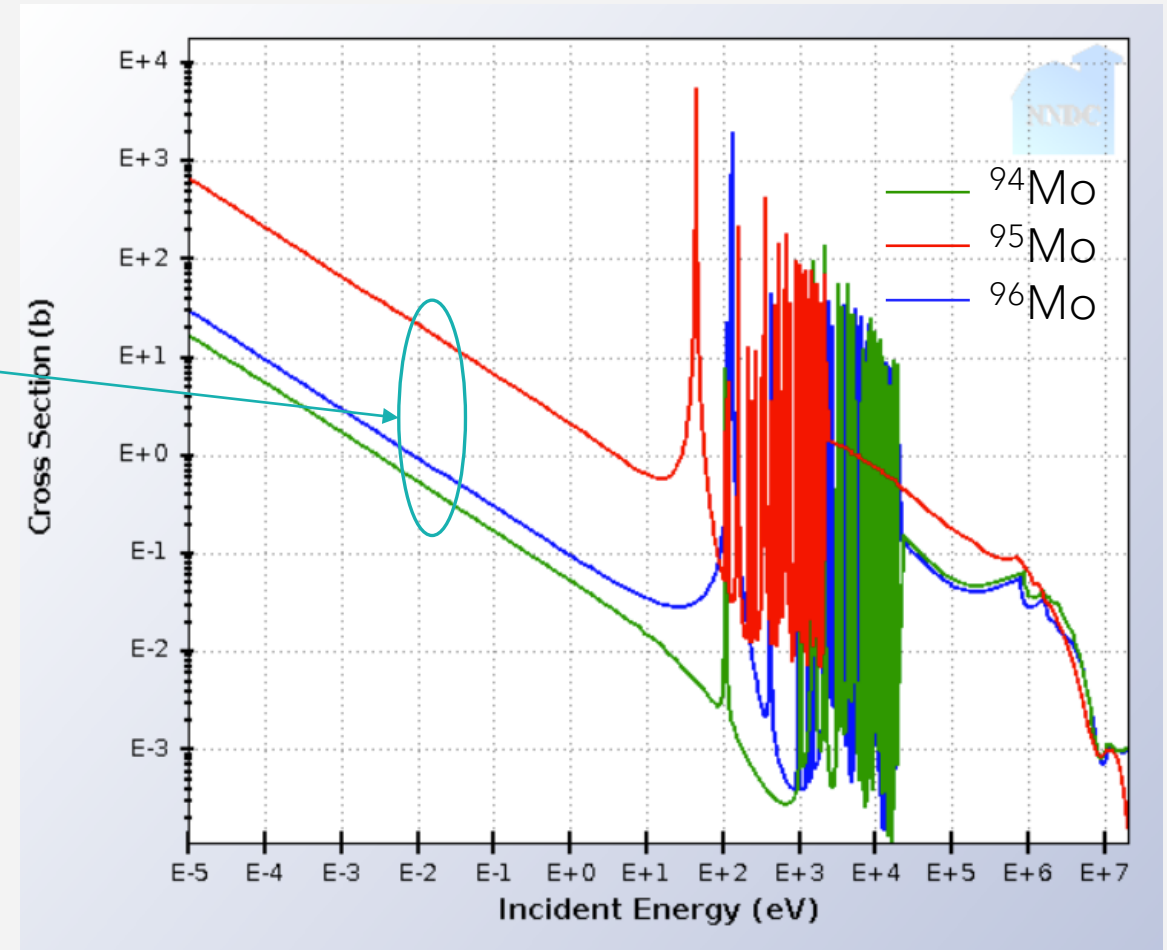
Capture cross section ENDF/B-VIII

Thermal cross section:

$^{94}\text{Mo} \sim 350\text{mb}$

$^{95}\text{Mo} \sim 13\text{b}$

$^{96}\text{Mo} \sim 620\text{mb}$



Transmission with enriched Mo

Transmission at 10 m station of GELINA

- Preliminary results of **transmission at 10 m** with enriched pellets;
- Resonance parameters from new compilation;
- Deviation on ^{95}Mo sample thickness from expected one;
- Abundance of biggest contaminants fitted with REFIT.

